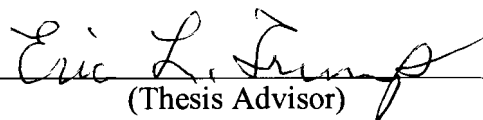


## AN ABSTRACT OF THE THESIS

Presented by Samuel Robert Smith Sarsah for Degree in Master of Science in Chemistry at the Department of Physical Sciences, Emporia State University, in May 2005.

TITLE: DESIGN AND SYNTHESIS OF AN OLIGONUCLEOTIDE-DOTA CONJUGATE

ABSTRACT APPROVED :   
(Thesis Advisor)

Chelates of the macrocycle DOTA and the  $Gd^{3+}$  ion serve as contrast agents for magnetic resonance imaging (MRI). MRI enhancement depends on the concentration of the metal complex agents at the target site. A higher concentration contrast agent gives better enhancement. This can be done by increasing the solubility of agents at the target site, or by increasing the number of metal complexes conjugated to a macromolecular agent, or by increasing the cellular uptake of the complex at the target site using molecules that bind to specific cellular receptors. Two  $Gd^{3+}$ -DOTA oligodeoxynucleotide conjugates were synthesized as potential MRI agents. Preparation of the oligodeoxynucleotide decamer was carried out by solid phase synthesis using an ABI 394 DNA Synthesizer.

The first oligonucleotide synthesized was destroyed during the purification step. A new DNA decamer oligonucleotide was synthesized and purified. The oligomer was cleaved from the column using ammonia/methylamine 1:1. Linkers that were conjugated to the oligomer were also synthesized in the lab and characterized with 60MHz NMR. However, the resulting oligomer was also denatured in the lab, so a new oligomer consisting of nine deoxythymidine nucleotides residue was made with the ninth

nucleotide derivatized with an amino hexane linker for coupling with DOTA-N-hydroxy-succinamide. This oligomer was purified on poly-pak column. Ultra violet spectroscopy showed a strong absorbance peak at 260nm. However the Gd-DOTA-oligomer conjugate did not have strong absorbance at 260nm. This was attributed to possible interference from Gd-DOTA complex.

We intended to couple the 15, 16-*O*-(isopropylidene)-4, 7,10,13-tetraoxahexadecylamide-folate liker to the Gd-DOTA-oligomer. The purpose is to deliver Gd<sup>3+</sup> selectively into tumor cells to enhance tumor imaging and thereby aid in the diagnosis of cancer. However, this was not successful.

# DESIGN AND SYNTHESIS OF AN OLIGONUCLEOTIDE–DOTA CONJUGATE

---

A Thesis

Presented to

The Department of Physical Sciences

EMPORIA STATE UNIVERSITY

---

In Partial Fulfillment

Of the Requirements for the Degree

Master of Science

---

by

Samuel Robert Smith Sarsah

May 2005

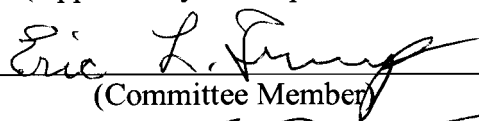
**Copyright 2005**

Samuel Robert Smith Sarsah  
ALL RIGHTS RESERVED

Thesis  
2000  
2



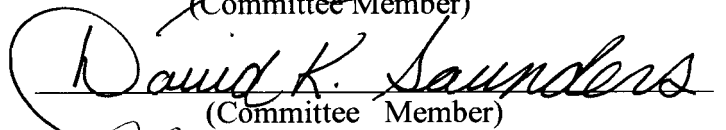
(Approval by the Department Chair)



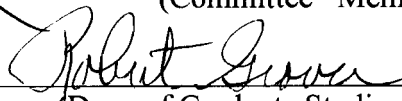
(Committee Member)



(Committee Member)



(Committee Member)



(Dean of Graduate Studies and Research)

## ACKNOWLEDGEMENT

My sincere thanks goes to all staff and members of Emporia State University Physical Science department especially Dr. Jim Roach, Dr. Michael Keck, Dr. Arthur Landis, Dr. Charles Greenlief and Dr. Eric Trump for their assistance in my research work as well as my graduate studies. I also thank Dr. Eric Trump, my research advisor, for all his efforts in making this work possible. I also wish to acknowledge financial support from an ESU Academic Success grant.

## TABLE OF CONTENTS

ABSTRACT	
ACKNOWLEDGEMENT	i
TABLE OF CONTENTS	ii
LIST OF FIGURES	vi
LIST OF TABLES	viii
LIST OF REACTION SCHEMES	viii
Keywords	ix
CHAPTER	
1 INTRODUCTION	1
2 HISTORY	2
3 NUCLEAR MAGNETIC RESONANCE	3
Requirements for MRI Contrast Agents	4
Relaxivity of Metal Complexes	4
Outer Sphere Relaxivity	8
4 LANTHANIDE METAL CHEMISTRY	10
Ionic of Gadolinium Complexes	10
Solution Properties	10
Hydrolysis and Precipitation	11
5 TOXICITY and CHELATE STABILITY	12
Stability Constants	13
6 BASIC REQUIREMENTS FOR BIFUNCTIONAL CHELATORS	19

	Denticity Requirements	20
	Ligand Framework	21
	Metal ion complexation	22
	Conjugated Groups	24
	Choice of Buffer	25
7	APPLICATIONS	26
	Renal Extracellular agents	26
	Hepatobiliary Agents	28
	Blood Pool Agents	30
8	MACROMOLECULAR CONJUGATES	32
	Dextrans	32
	Dendrimers	34
	Biomolecules (Protein, Polysaacharides, Nucleic Acids)	36
9	TUMOR TARGETING	38
	Tumor Receptors	38
	Folic acid Receptors	38
	Qualities of a good folated agent	39
	Use of Polyethylene Glycol (PEG) linkers and their limitations	39
	Mechanism of folate receptor mediated endocytosis	42
	Applications of folated agents in tumor targeting	43
10	SOLID PHASE OLIGONUCLEOTIDE SYNTHESIS	48
11	SUMMARY OF THESIS	51

12	EXPERIMENTAL	52
	Materials	52
	Synthesis of 5-Methoxycarbonylvinyl- 2`-deoxyuridine	52
	Synthesis of 5-Methoxycarbonylvinyl`-5`- <i>O</i> -(dimethoxytrityl)- -2`-deoxyuridine	53
	Synthesis of 5-[N (6-Aminohexyl)-3-(E)-acrylamido]-5`- <i>O</i> - (dimethoxytrityl)-2`-deoxyuridine	53
	Synthesis of 5-[N(6-Aminohexyl)-3-(E)-acrylamidotrifluoroacetyl]-5`- <i>O</i> -(dimethoxytrityl)-2`-deoxyuridine	54
	Synthesis of 5-[N(6-Aminohexyl)-3-(E)-acrylamidotrifluoroacetyl]-5` <i>O</i> -5-(dimethoxytrityl)-3`-(2-cyanoethyl-diisopropyl-chlorophosph- oramidite) -2-` deoxyuridine	54
	Automated DNA Synthesis	55
	DNA Conjugation and Purification	56
	Preparation of Bicarbonate (pH 9) Buffer	56
	Purification of DNA	56
	Preparation of DNA DOTA linker	57
	Preparation of Gd(III)Chloride aqueous solution	57
	Preparation of EDTA solution	57
	Preparation of Gd-DOTA DNA conjugate	57
	UV Measurements	57
	Gel electrophoresis	58
	Preparation of Solutions	58

30%Acrylamide	58
Buffer	58
10% Ammonia persulfate	58
Acrylamide–Urea Polymer	58
DNA Electrophoresis	59
Synthesis of 6-Formylpterin	59
Synthesis of N-Isobutyryl-6-formylpterin	60
Synthesis of folic acid Succinamide Ester	60
Synthesis of 15, 16– <i>O</i> -(isopropylidene)-4, 7, 10, 13-tetraoxahexadecylamine folate ester	61
13 RESULTS AND DISCUSSION	62
14 CONCLUSION	74
REFERENCES	75

## LIST OF FIGURES

Figure	Content	Page
1	a) Gd-DOTA complex	6
	b) Interactions of water molecules with MRI metalcomplexes	7
2	Protected derivatives of DOTA	20
3	Different ways of conjugating macromolecules to DOTA ligand	21
4	Mechanism of a) metal ion ( $Y^{3+}$ ) complexation by singly protonated DOTA in neutral solutions and b) deprotonation of ligand nitrogen by an $OH^-$ ion prior to $Gd^{3+}$ complexation.	22
5	Gd-DOTA lipophilic agents with long hydrocarbon esters	29
6	a) Synthesis of PL-DTPA	31
	b) Synthesis of PL-DOTA	31
	c) Synthesis of PL- Gd(III)DOTA conjugated to HSA	31
7	a) Synthesis of CMDA-DTPA	34
	b) Macrocyclic CMD-A2-Gd-DOTA	34
8	Generation-2-PAMAM thiourea dendrimer	36
9	Poly (L-glutamic acid) –cystamine –[Gd(III)DOTA]	37
10	HS-distearoylphosphatidylethanolamine (DSPE) liposomal agent linked with PEG.	41
11	Liposomal Gd-DTPA agent conjugated to E-selectin antibodies for targeting HUVEC	42
12	Folate receptor endocytosis mechanism for delivery of boronated. Agents. For intracellular targeting of DNA of tumor cells is illust rated below. Encapsulated boronated agent is then released into the cytosol via endosomal escape and bound to the DNA in the cellular nucleus.	43

13	Gadolinium hexanedione (GdH) complex. b) Structure of folate –PEG-DSPE-synthesized by linking folic acid to DSPE via a PEG spacer (M.W. 3350).	44
14	Synthesis of folic acid conjugated to DSPE via PEG spacer.	45
15	Structure of carboplatin (a) and folic acid (b).	46
16	Synthesis of folic acid conjugated to deferoxamine.	46
17	DNA synthesis by standard four step phosphoramidite process	48
18	a.) Synthesis of phosphoramidite nucleotide	49
	b) New two step synthesis of ODN	50
19	Structure of compound 9	67
20	U.V. Spectrum of denatured DNA oligomer	68
21	U.V. Spectrum of new oligo (active)	70
22	U.V.spectrum of oligomer coupled to Gd-DOTA complex	70
23	U.V. Spectrum of Gd-DOTA Complex	71

## LIST OF TABLES

Page

Table 1. Stability constant for cyclic and acyclic complexes of Gd (III)	18
--	----

## LIST OF REACTION SCHEMES

Page

SCHEME I .....	63
SCHEME II .....	64
SCHEME III .....	65
SCHEME IV .....	66
SCHEME V .....	69
SCHEME VI .....	72
SCHEME VII .....	73

## Keywords or abbreviation

DOTA.....	1,4,7,10-tetraazacyclododecane-N,N',N'',N'''-tetraacetic acid.
DTPA .....	Diethylenetriaminepentaacetic acid
MRI .....	Magnetic resonance imaging
HAS .....	Human serum albumen
BSA .....	Bovine serum albumen
FR .....	Folate receptor
FA .....	Folic acid
NMR .....	Nuclear magnetic resonance
TCA .....	Trichloroacetic acid
TLC .....	Thin layer chromatography
DMSO .....	Dimethylsulfoxide
DMSF .....	N, N'-dimethylformamide
ODN .....	Oligodeoxynucleotide
DNA .....	Deoxyoligonucleotide
PEG .....	Polyethyleneglycol
PL .....	Polylysine
mPEG .....	Methoxy-PEG
ARCO .....	Aryloxy carbonyl
DMT .....	Dimethoxytrityl
DSPE .....	Distearoylphosphatidylethanolamine
NHS .....	N-Hydroxysuccinamide
PAMAM .....	Polyamidoamine
DAB .....	Diaminobenzene
FDA .....	Food and Drug Administration
NOTA .....	1,4,7-triazacyclononane-N,N',N''-triacetic acid
THAM .....	Tris(hydroxyethyl)amine
TEA .....	Triethylamine
TFA .....	Trifluoroacetic acid

## 1 INTRODUCTION

Magnetic Resonance Imaging (MRI) is a technique that uses the magnetic effect on electrons and protons by chemical agents to image body tissues for clinical diagnosis. In addition to MRI, other techniques used for diagnosis include X-rays, Computer Tomography, and staining techniques. MRI has several advantages over other techniques. These include high sensitivity, minimal side effects, and the ability to image both hard and soft tissues. MRI primarily relies on the magnetic effect on the relaxation of water protons to provide NMR images of internal body tissues, organs or cells. Differences in the structure and composition of metal chelate complexes (contrast agents) lead to variations in the ways that they interact with different body molecules. This leads to differences in the proton relaxation rates of body water molecules that are coordinated to the metal in the complex and enhances the image of targeted tissues having high selectivity for the MRI agent. Surrounding tissues are not enhanced. Certain receptors, especially folic acid receptors, are more highly enriched in diseased tissues or cells than in normal cells. Therefore, MRI agents can be developed that allow exclusive targeting of certain body tissues. Diagnosis can be made easily, since images of normal organs or tissues can be differentiated from abnormal or diseased ones. Certainly, knowledge for developing agents that will give the best image enhancement with minimal side effects from toxicity is essential. It is incumbent upon chemists to determine the composition, structure, and dosage required for such agents to be used safely and effectively. This thesis reports the synthesis of a Gd-DOTA complex conjugated to a nine unit deoxythymidine oligonucleotide by an amide condensation with a hexamino linker.

## 2 HISTORY

Paramagnetic enhancement of water proton relaxation rates was first observed in ferric nitrate salts by Bloch (103). Proton Relaxation Enhancement (PRE) experiments have been carried out by Eisenger, Shulman, and Blumberg by increasing the rotational correlation time to enhance water proton relaxation from paramagnetic ions bound to DNA (98). In 1973 it was reported that longitudinal relaxation rates ( $1/T_1$ ) of water protons in canine myocardial tissues (104) were enhanced relative to infarcted tissues by the preferential localization of  $Mn^{2+}$  ions in the myocardial tissues. The infarcted zone was then distinct from the normal myocardial zone. The technique was extended to humans in 1977 and confirmed in other experiments done on dog hearts (105,106).

Ferric chloride administered to enhance the gastrointestinal tract was the first human application of MRI carried out by Young and his co-workers (107). Gadolinium (III) was the first paramagnetic agent to be tried for patient diagnosis. Gadolinium (III) diethylenetriaminepentaacetate  $[Gd(DTPA)(H_2O)]^{2-}$  was administered intravenously to enhance lesions in the regions of cerebral capillary breakdown in patients with cerebral tumors (1).

### 3 NUCLEAR MAGNETIC RESONANCE

MRI (Magnetic Resonance Imaging), previously known as Nuclear Magnetic Resonance Imaging, requires that atomic nuclei have odd or half nuclear spins. Relaxation of excited hydrogens of water molecules is the basis of medical MRI (45). Spins of atomic nuclei can exist in two energy states, namely, the ground state and the excited state. At every temperature there are a number of spins directed towards the applied field (lower state) or against the field. The frequency of the spin of atomic nuclei in a magnetic field strength  $\mathbf{B}$  can be expressed as:

$\mathbf{v} = \gamma\mathbf{B}$  where  $\mathbf{v}$  is the gyromagnetic ratio and  $\gamma$  is the gyromagnetic ratio (144).

The atomic nuclei will absorb photons of energy corresponding to the energy gap between the ground and excited states. This is typically in the range of 60 to 800MHz for NMR spectroscopy and 15 to 80MHz for MRI hydrogen imaging. The energy  $E$  is described by ;

$E = h\nu = h\gamma\mathbf{B}$  where  $h$  is Planck's constant.

At equilibrium, the vector direction of net magnetization of the interaction of magnetic force due to spins of the atomic nuclei and that of the applied external magnetic field is directed towards the Z-axis (longitudinal component). There is no transverse component (x or y).

If the radiofrequency energy that matches the energy gap between spin states is supplied, the energy is absorbed to increase the spin states of the atomic nuclei. This changes the direction of the net magnetization from the Z-axis and possibly to zero if enough energy is supplied to saturate the system. The energy is released as nuclei return to the ground state. This can be converted into signals that give information about the chemical environment of the spinning nuclei. The time

constant that describes the return of nuclear spins to equilibrium along the X-Y plane is called the Spin-Spin Relaxation Time ( $T_2$ ). Molecular interactions and external magnetic field variations leads to decay of transverse magnetization.

Processes leading to transverse and longitudinal relaxation occur simultaneously, but  $T_2$  is always less than or equal to  $T_1$  (26, 28). The energy emitted as the nuclei return to equilibrium in both  $T_1$  and  $T_2$  can be converted to electrical signals and used for analyzing the chemical environment of the protons (27,45).

## **REQUIREMENTS FOR MRI CONTRAST AGENTS**

In addition to biocompatibility, water solubility, and shelf stability, the other requirements for good agents are relaxivity, specific *in vivo* distribution, *in vivo* stability, excretability, and lack of toxicity (1). Agents should be designed to satisfy clinical and FDA (Food and Drug Administration) standards (13). A good MRI agent must have high and fast uptake at the target site, high target to background ratio, long residence time at the target site, and fast excretion from the body. The high uptake at the target site and fast renal clearance improves the target-to-background enhancement ratio and reduces toxicity to other normal organs such as kidneys, liver, and bone marrow. Agents must have high purity and high kinetic and thermodynamic stability in solution. MRI agents are usually made (complexed) immediately before injection (13).

## **RELAXIVITY OF METAL COMPLEXES**

$Gd^{3+}$  is more widely used as an MRI agent than other metal agents such as  $Fe^{2+}$  or  $Mn^{2+}$ . Highly paramagnetic Gd(III), with seven unpaired electrons (spin state 7/2) leads to a much slower electronic relaxation rate. Unpaired electron spins reinforce each other. The dipolar interaction between unpaired  $Gd^{3+}$  electrons

and the water nuclei causes relaxivity to increase, since the water proton frequency is closely tuned with that of the  $Gd^{3+}$  electrons (109).

Contrast agents are chemicals that can promote marked changes in the relaxation rate of tissues protons (99). Positive contrast agents are paramagnetic complexes, mostly containing Gd(III) or Mn(II) ions, which affect relaxation rates of bulk water protons through the exchange of water molecules in coordination spheres.

MRI depends on the longitudinal relaxation rate ( $1/T_1$ ) and the transverse relaxation rate ( $1/T_2$ ) of water protons. Longitudinal and transverse relaxation rates of solvent nuclei are both increased by paramagnetic agents. The increase in  $1/T_1$  and  $1/T_2$  is about the same for these agents and is best used to give brighter  $T_1$ -weighted images since  $1/T_1$  is usually significantly longer than  $1/T_2$  in most targeted biological tissues, resulting in a higher percentage change for  $1/T_1$  than for  $1/T_2$  (99).

Negative contrast agents, e.g., iron oxide particles, are used to shorten  $1/T_2$ , (or increase  $T_2$ ), leading to improved contrast and reducing the water signal in  $T_2$ -weighted images. Large changes in magnetic susceptibility around the particles determine their function (1, 99). This can be used for paramagnetic lanthanides confined in microcompartments, such as capillary vessels. Chemicals containing mobile protons may act as  $T_2$  agents through decreased water proton relaxation time by an exchange process (99). The observed relaxation rate is a sum of diamagnetic and paramagnetic components:

$(1/T_i)_{obs} = (1/T_i)_d + (1/T_i)_p$  ( $i = 1$  or  $2$ ) where 1 or 2 refers to longitudinal and transverse relaxation respectively) (1). The term  $(1/T_i)_{obs}$  is the observed solvent relaxation rate in the presence of paramagnetic species,  $(1/T_i)_d$  is diamagnetic

solvent relaxation rate in absence of paramagnetic species, and  $(1/T_i)_p$  is the additional paramagnetic contribution.

Relaxivity ( $R$ ) (measured in  $M^{-1}s^{-1}$  or commonly  $mM^{-1}s^{-1}$ ) is the slope of the plot of observed solvent relaxation rate  $(1/T_i)_{obsv}$  against concentration of paramagnetic species  $[M]$ .  $(1/T_i)_{obsv} = (1/T_i)_d + R_i [M]$  ( $i = 1$  or  $2$ ). Longitudinal relaxivity  $r_1$  refers to change in the  $1/T_1$  per millimolar of agent  $r_2$  while transverse relaxivity accompanies the change in  $1/T_2$ . The ratio  $r_1/r_2$  ratio is usually 1 to 2 for  $T_1$  agents such as  $Gd^{3+}$ , but 10 or more for  $T_2$  agents such as iron oxide (2).

Large fluctuating local magnetic fields near paramagnetic centers needed for solvent nuclei relaxation diminish with distance. Of vital consideration is the random translational diffusion of the solvent molecules and complex, as well as specific chemical interactions (H-bonding, Van der Waals, etc.) that bring solvent molecules within 0.5nm of the metal ions (1).

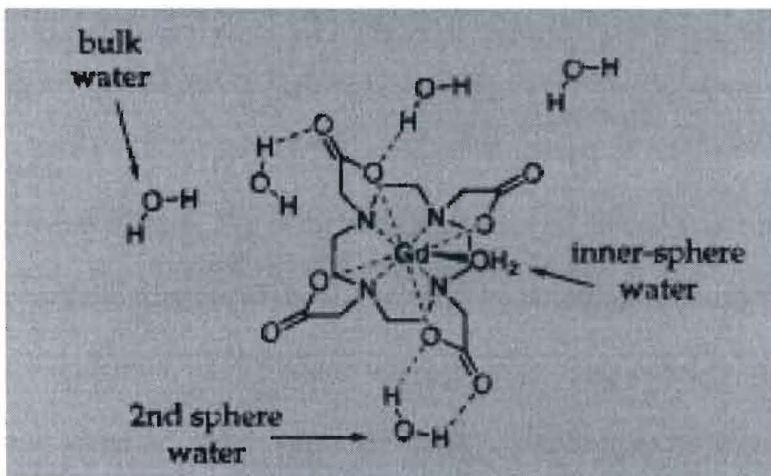


**Figure 1a.** Interactions of water molecules with Gd-DOTA complex

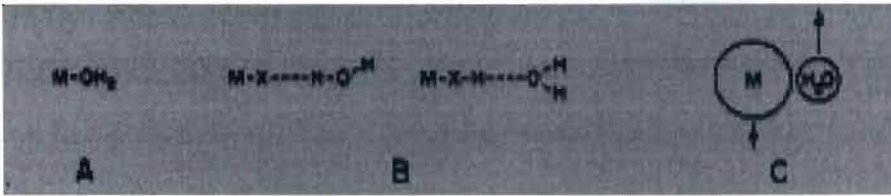


**Figure 1b.** Interactions of water molecules with MRI metal complexes

Two types of interactions are considered, namely, direct coordination of water molecules to metal ions (Figure 1) which undergo periodic exchanges with molecules in bulk solvent (inner sphere relaxation) (2), and dipolar interactions from hydrogen bonding of bulk water molecules with atoms of chelates and metal atoms (second sphere relaxation), and the translational diffusion of water molecules past the chelate. Second sphere relaxation and translational diffusion of water molecules past the chelate all constitute Outer Sphere Relaxation (110,111).

Total relaxation that is measured is a sum of inner and outer sphere relaxation

$$(1/T_i)_p = (1/T_i)_{\text{inner sphere}} + (1/T_i)_{\text{outer sphere}} \quad (i = 1 \text{ or } 2),$$

where  $(1/T_i)_p$  is the total relaxivity of the paramagnetic agent.

Image enhancement is largely dependent on the longitudinal relaxation enhancement which is described in the equation;  $(1/T_i)_{\text{inner sphere}} = P_m q / (T_{1m} + \tau_m)$ , where  $P_m$  is the mole fraction of metal ions,  $q$  is number of water molecules bound per metal atom,  $T_{1m}$  is the relaxation time of bound water protons, and  $\tau_m$  is the residence lifetime of bound water. The Solomon-Bloembergen equation (98) accounts for relaxation rate of bound water protons. This consists of dipolar (through – space) and scalar or contact (through bonds) contributions as described in the following expression:

$$\frac{1}{T_{1M}} = \frac{2}{15} \frac{\gamma_I^2 g^2 S(S+1) \beta^2}{r^6} \left[ \frac{7\tau_c}{(1 + \omega_S^2 \tau_c^2)} + \frac{3\tau_c}{(1 + \omega_I^2 \tau_c^2)} \right] + \frac{2}{3} S(S+1) \left( \frac{A}{\hbar} \right)^2 \left[ \frac{\tau_c}{1 + \omega_S^2 \tau_c^2} \right]$$

where  $\gamma$  is the proton gyromagneto ratio,  $g$  is electronic  $g$  factor,  $S$  is total electron spin of metal ion,  $\beta$  is Bohr magneton,  $r$  is proton – metal ion distance,  $\omega_s$  is electronic Larmor precession,  $\omega_i$  is proton Larmor frequency and  $(A/H)$  is electronic -nuclear hyperfine coupling constant.

In the following expression,

$$1/\tau_c = 1/T_{1e} + 1/\tau_m + 1/\tau_R \qquad 1/\tau_e = 1/T_{1e} + 1/\tau_m$$

$\tau_e$  and  $\tau_c$  are overall correlational time for contact relaxation and dipolar relaxation respectively.  $T_{1e}$  is longitudinal electronic spin relaxation time,  $\tau_m$  is water residence time and  $\tau_R$  is the rotational tumbling time of the entire metal-water unit (112-116).

The  $\tau_R$  is expressed by the equation  $\tau_R = 4\pi a^3 \eta / (3kT)$ , where  $a$  is the radius of the metal complex as a sphere,  $\eta$  is viscosity,  $T$  is absolute temperature, and  $k$  is Boltzmann's constant

## **OUTER SPHERE RELAXIVITY**

Inner sphere relaxivity is high for open chain aquo metal ion complexes because of their ability to coordinate a high number of water molecules, which increases the rotational tumbling time of complexes, compared to metal ions with no bound water molecules  $q = 0$  (1). However, outer sphere relaxivity becomes dominant for the highly stable multidentate ligands (such as DOTA and other low molecular weight macrocyclic complexes), due to the reduced the number of coordinated water molecules, which causes less inner sphere relaxation. Total relaxivity is dominated by outer sphere relaxation for macrocyclic multidentate ligands.

In the absence of chemical or electronic interactions, outer sphere relaxivity is modulated by electronic–nuclear dipolar interactions from the translational diffusion of

water molecules around the complex and by field energy fluctuations (117,118).

The general equation (118) for outer sphere relaxivity is given as:

$$\left[ \frac{1}{T_1} \right]_{\text{outer sphere}} = \frac{C r N_S \gamma^2 \gamma_E^2 \hbar^2 S(S+1)}{d^6 \tau_D} [7I(\omega_S \tau_D T_{1e}) + 3I(\omega_T \tau_D T_{1e})],$$

where C is a numerical constant (different in different equations),  $N_S$  is the number of metal ions per  $\text{cm}^3$ , d is distance of the closest solvent molecule to the metal complex, and  $\tau_D$  is the relative translational diffusion time,  $\tau_D = d^2/[3(D_1 + D_s)]$ , where  $D_1$  and  $D_s$  are the diffusion coefficients of water and the metal complex, respectively. These diffusion coefficients are described by the equation  $D = KT/(\delta\pi a\eta)$ , where  $\eta$  and  $a$  are viscosity of the medium and the molecular radius of complex taken as rigid sphere, respectively.

## 4 LANTHANIDE METAL CHEMISTRY

### IONIC NATURE OF Gd-CHELATE COMPLEX

The most common oxidation state of lanthanide metal ions is +3. Unlike d-block transition metals, the 4f electrons of lanthanides are inner electrons shielded from external influences by overlying  $5s^2$ ,  $5p^6$ , and  $6s^2$  electrons shells (74). The ligand field effect is relatively weak and the magnetic properties of metal ions are not significantly affected by the coordination environment. The 4f electrons are not involved in bonding, therefore interactions between donor atoms and the lanthanide metal ions are predominantly ionic (13).

The large sizes of lanthanides (such as gadolinium) favor high coordination numbers in aqueous media. All  $Gd^{3+}$  based chelates currently approved for use in MRI are nine-coordination complexes in which a ligand occupies 8 binding sites at the metal center and the ninth coordination site is occupied by a solvent water molecule (13). The ionic nature of bonds in Gd-DOTA chelates results in longer bond distances for M-N bonds than for M-O bonds, e.g.  $Gd-N = 0.264-0.265\text{nm}$  and  $Gd-O$  (carboxylate) =  $0.231-0.238\text{nm}$  (15).

### SOLUTION PROPERTIES

The naked +3 state that is most often written to represent lanthanide metal ions is oversimplified. Metals exist in complexed form bonded with water molecules in aqueous solution. Coordination number (number of water molecules bonded directly to metal ions) is similar to the number of donor atoms found in its metal chelates in the solid state and depends largely on the size of the metal ion (74). The coordinated water molecules are replaced by chelating agents during metal chelate complex formation. Common coordination numbers for lanthanides range from 7 to 10,

due to their large size.  $Gd^{3+}$  is 8 coordinate and is more accurately written as  $[Gd(H_2O)_8]^{3+}$  (26). Metal ions such as  $Gd^{3+}$  have a coordination number of 9. Gd-DOTA is an octadentate complex, but  $[Gd(DOTA)(H_2O)]^-$  is nonadentate complex. In all but  $Gd^{3+}$ , metal-water bonds are labilized by substitution of water with stronger anion donor ligands (13).

## **HYDROLYSIS AND PRECIPITATION**

Hydroxides, phosphates, and carbonates easily precipitate lanthanide metal ions in aqueous solutions. Phosphates and carbonates compete for metal ions in the chelate-conjugated complexes, but the competition from hydroxide ion is not significant, since its concentration is much lower *in vivo*. The high affinity of lanthanides for phosphate anions may explain their affinity for bones (13).

## 5 TOXICITY AND CHELATE STABILITY

*In vivo* stability and tissue clearance behavior can affect the toxicity of an agent. *In vivo* dissociation of a complex should not occur, since the free metal ions and free ligands are more toxic at doses used for diagnosis. Excretion of the MRI agent must occur within hours after administration (2).

Because  $\text{Gd}(\text{H}_2\text{O})_8^{3+}$  is very highly toxic *in vivo*, the metal must be complexed before administering to patients (14). The free metal ion and the free ligand are more toxic than the metal complex. This is due to the fact that both metal ion and ligands lose their ability to coordinate upon forming a complex and this markedly reduces any chances of binding to proteins or membranes by electrostatic or hydrogen bonding interactions or by covalent bonding. *In vivo* dissociation of complexes before excretion directly relates to the degree of toxicity. The toxicity of  $\text{Gd}^{3+}$  stems from it binding to serum proteins and its strongly irreversible incorporation into bone. This occurs because  $\text{Gd}^{3+}$  can bind to  $\text{Ca}^{2+}$  sites, often with higher affinity, due to its greater charge /radius ratio (1).

Detection of  $\text{Gd}^{3+}$  is usually done by using ICP atomic emission or by gamma counting for Gd-153 or Gd-159 labeled complexes in skeletal tissues (120-122). The free ligand toxicity stems from the ability to bind very important free metal ions such as  $\text{Ca}^{2+}$ ,  $\text{Mg}^{2+}$ ,  $\text{Na}^+$ ,  $\text{K}^+$  --all of which are needed for body metabolism. Therefore, the stability of complexes is essential in preventing dissociation into free  $\text{Gd}^{3+}$  and chelate. Toxicity from intact metal complexes stems from various causes. For example, in the case of relatively non-toxic hydrophobic chelates such as  $[\text{Gd}(\text{DOTA})(\text{H}_2\text{O})]^-$ , injection of large doses of the ionic complex with its counter ions increases the concentration

of extracellular fluid compared to the intracellular fluid. The large osmotic gradient (or difference in osmolality) draws water out of cells, leading to cell damage or circulatory malfunction (75,79).

Binding of predominantly negatively charged macromolecules (such as DNA, RNA etc) and cell surfaces by cations also leads to toxicity. Administered MRI agents should remain in the body for minutes or hours before excretion. Therefore, the stability required for this short period of time is kinetic, not thermodynamic (123,124). The correct multidentate ligand is required to ensure kinetic stability. However, thermodynamic stability merely shows the direction of the metal ion complexation reaction, and not the rate of dissociation of the metal complex.

Competition from native cations and anions in the body will result in dissociation of the complex. Macrocyclic agents such as DOTA exhibit significantly less acid catalyzed release of ions *in vivo* (125-128) than acyclic agents. However, some agents reside in the body long enough to interact with cell surface receptor molecules. This can lead to toxicity when these agents are internalized into the body cells. Thus, hepatobiliary and tumor agents must have high kinetic and thermodynamic stability (129-131). Gd-DOTA complexes are thermodynamically and kinetically inert (132,133). The Gadolinium complex must be highly inert to withstand attack from nucleophiles or electrophiles *in vivo*. The charged metal complex will be repelled at the charged cell surface. Thus, it is unlikely that it will enter cells. The cage-like chelated ion has less opportunity for binding to donor groups in proteins and enzymes.

## STABILITY CONSTANTS

Major ways of expressing relative stabilities of Gd<sup>3+</sup> complexes include:

- 1) The thermodynamic stability constant,  $K_{ML}$ , (stability of complex in the basic conditions in which it was formed).

2) The conditional stability constant,  $K_{ML}^*$ , or the stability constant at pH 7.4.

(It is less than the overall stability constant due to competition between  $H^+$  and  $Gd^{3+}$  for ligand at this pH).

3) The selectivity constant ( $\log K_{sei}$ ) of the  $Gd^{3+}$  complex, which is the stability constant of the complex formed in the presence of endogenous metal ions.

This is the stability constant corrected for competition between endogenous metal ions and  $H^+$  (82). Higher selectivity for  $Gd^{3+}$  implies that the endogenous metal ions are less able to displace  $Gd^{3+}$  from the chelate.

4) The degree of conversion of free ligand to chelate complex ( $K_{sol}$ ).

Equilibrium between  $Gd^{3+}$  and competing endogenous cations and anions potentially leads to dissociation of  $Gd^{3+}$  from the complex. The thermodynamic stability constant ( $K_{GdL}$ ) is large for all clinically viable agents. For example,  $[Gd(DOTA)]^-$  gives a value of  $10^{25.6}$ . The equilibrium shift is towards complexation, with virtually no free metal ion or ligand present (1,2,13). The equilibrium is described by the following expression;



A high pH medium is usually preferred for complexation. However, in neutral or physiological medium (pH 7.4), protons compete with the metal ions for ligand binding sites. This is described by the equation;

$$K_{mL}^* = K_{ML} / [(1 + K_1[H^+] + K_1K_2[H^+]^2 + \dots + K_1K_2K_n[H^+]^n)]$$

$K_1, K_2, K_3, \dots, K_n$  are stepwise dissociation constant of ligand.  $K_{mL}^*$  is the conditional (or pH dependant) stability constant (13).

$K_{mL}$  is also known as the formal stability constant,  $K_{mL}^*$ , of chelates measured at

pH 7.4. Conditional (ligand protonation) constants (pH 4 and 7.4) and thermodynamic stability constants of  $Gd^{3+}$ -DOTA complexes have been reported (10).

The following equations describe the conditional stability constant;

$$\text{Log } K_{mL}^* = 11.2 \pm 0.5 \text{ at pH 4 and } 18.6 \text{ at pH 7.4 and } \log K_{mL} = 25.3 \text{ at } 25^\circ\text{C}$$

$$K_{ml} = K_{ml}^* (1 + K_1[H^+] + K_1K_2[H^+]^2 + \dots + K_n[H^+]^n),$$

where  $K_1, K_2, K_3, \dots, K_n$  are stepwise protonation constants of ligand. Conditional stability is therefore very important in biological studies. Proton competition under physiological conditions depends on the basicity of the ligand (10).

Competition by  $Ca^{2+}$ ,  $Cu^{2+}$ ,  $Zn^{2+}$ ,  $PO_4^{3-}$ ,  $CO_3^{2-}$ ,  $OH^-$  and  $H^+$ , with  $Gd^{3+}$  and ligand depends on the relative affinity of ligand for these metal ions (stability constants) and  $H^+$  (ligand protonation constants) and the relative affinity of  $PO_4^{3-}$ ,  $CO_3^{2-}$ , and  $OH^-$  for  $Gd^{3+}$  ions compared to the ligand. Low solubility products of  $Gd(PO_4)$  and  $Gd(OH)_3$  are sufficient enough to cause precipitation of  $Gd^{3+}$  from the chelates with relatively low stability constants (and kinetic inertness).

$K_{sei}$  values for DOTA, and Gadolinium-1, 4, 7-triazacyclononane-N, N', N''-triacetic acid [ $Gd(NOTA)$ ] are 8.3 and  $-1.94$ , respectively. This means that DOTA has higher selectivity for Gd *in vivo* than NOTA (5,6,8,122). *In vivo* metal displacement and hence toxicity will be higher for NOTA than DOTA (9,82). At equilibrium, a ligand with a high gadolinium selectivity factor ( $K_{sei}$ ) binds Gd(III) more strongly in the presence of competing metal ions [ $Ca^{2+}$ ,  $Cu^{2+}$ , and  $Zn^{2+}$  etc] than ligands with a lower selectivity factors ( $\log K_{sei}$ ). Selectivity is not applicable to Gd(III) complexes of macrocyclic polyamino carboxylate ligand such as DOTA, because of their high thermodynamic and kinetic stability. However, it is applied for complexes in

which dissociation and substitution are so rapid that transmetalation occurs *in vivo*.

Gd-DOTA complex is thermodynamically stable and kinetically inert (2).

Different donor atoms have different affinities for the lanthanide ions in the complex.

In general, electron donating groups attached to the donor atom of the chelate increases the donor strength (2, 97). Dissociation of the complex, is influenced by many factors. One of these is competition for coordination binding sites of the chelate by water protons and abundant metal ions such as  $\text{Ca}^{2+}$ ,  $\text{Cu}^{2+}$ ,  $\text{Zn}^{2+}$  and  $\text{Fe}^{3+}$  in the bloodstream. Another factor is competition of the ligand for the metal ions by hydroxides, phosphates, and native chelators such as amino acids and transferrin in the bloodstream (88). If an anion forms a precipitate, a chelate with a high thermodynamic stability could solubilize that precipitate. This is described by the expression;  $K_d = K_a/K_{mL}$  where  $K_d$ ,  $K_a$  and  $K_{mL}$  are the dissociative rate constant, associative rate constant, and thermodynamic associative constant respectively (1,13).  $\text{Gd}^{3+}$  forms thermodynamically stable complexes with phosphates and carbonates, while  $\text{Fe}^{3+}$  forms complexes with hydroxides. The  $\text{Mn}^{2+}$  generally do not form appreciable complexes with these anions (54). A high thermodynamic stability of complex to precipitate in serum might imply that the ligand can solubilize the ion from its precipitate. This can be described by the equation  $K_{sol} = [\text{ML}]/T_L$ , where  $K_{sol}$ ,  $T_L$ , and  $[\text{ML}]$  are the degree of conversion of free ligand to metal chelate, total concentration of ligand, and concentration of the complex respectively (13).

Low  $K_{sol}$  means ligands cannot solubilize the ion. The complex will be unstable because the metal forms a highly stable precipitate with other oppositely charged ions. Very high  $K_{sol}$  implies that the metal-ligand complex is thermodynamically stable and that the metal ion will not precipitate in the presence

of other ions (13).  $[\text{Gd}(\text{DOTA})(\text{H}_2\text{O})]^-$  is stable *in vivo* (29). The free ligand concentration is consumed in the  $\text{Ca}^{2+}$  5mM physiological medium due to high  $K_{\text{mL}}$  of  $[\text{Ca}(\text{DOTA})]^{2+}$  complex. Therefore,  $K_{\text{sol}}$  is lower than expected, despite a higher  $K_{\text{mL}}$  for the Gd-DOTA complex. The conformational stability of  $[\text{Gd}(\text{DOTA})(\text{H}_2\text{O})]^-$  and its macrocyclic nature renders its dissociation kinetics very slow. The  $K_{\text{d}}$  is  $10^{-5} \text{ M}^{-1}\text{s}^{-1}$  for acid-catalyzed dissociation. At pH 1, the complex has a half-life of approximately 11 days and at pH 6 and its half-life is over 2000 years (102). This shows that thermodynamics alone cannot be used to predict the biological properties of the complex (1). Stability or dissociation of chelates depends on charge density, ring size, number of donor atoms, and ring and side arm substituents (6,81,97). Macrocyclic polyamino complexes show variations such as preorganization of free ligand, conformation, cavity size, ligand basicity and rigidity (4,7,80,16).

Generally, the thermodynamic and kinetic stability of metal-ligand lanthanide complexes of hepta-, and octadentate macrocyclic polyaminocarboxylates increases with increasing charge density and with smaller ionic radii of the metal ions, even though this does not correlate well with  $[\text{Gd}(\text{DOTA})]^-$  complexes (6,15,78).

Multiple regression analysis from results of calculations of quantum mechanical descriptors and topological indices has been used to investigate the relationship between the structures of ligands and their stability constants of gadolinium (III) complexes. A mathematical model was proposed to predict the properties of proposed and existing compounds (Table 1) (18).

**Table 1. Stability constant for cyclic and acyclic complexes of Gd (III)**

no.	ligand	logK <sub>0a</sub>	no.	ligand	logK <sub>0a</sub>
1	DTPA-BMEA	16.84	15	DTPA-BAM	15.39
2	DTPA-BMMEA	17.68	16	DTPA-cis <sup>2+</sup> -CBAM	15.56
3	DTPA-BMA	16.85	17	DTPA-OAM	17.44
4	DTTA-BM	13.12	18	NOTA	13.70
5	DTTA-HP	23.65	19	DETA	15.10
6	DOTA	25.30	20	Me <sub>2</sub> -DETA	10.40
7	DO3MA	25.30	21	PC2A	16.60
8	DO3A	21.10	22	BP2A	14.50
9	DOTP	28.80	23	N <sub>3</sub> O <sub>4</sub> -L <sub>1</sub>	16.27
10	HP-DO3A	23.80	24	N <sub>3</sub> O <sub>5</sub> -L <sub>1</sub>	11.49
11	HP-DO3A	23.90	25	N <sub>3</sub> O <sub>5</sub> -L <sub>2</sub>	18.07
12	HE-DO3A	22.30	26	N <sub>3</sub> O <sub>5</sub> -L <sub>2</sub>	17.23
13	DTPA-EAM	11.15	27	TTAHA	19.00
14	DTPA-PAM	14.49	28	PEDTA	15.56

The basicity of ligand nitrogen (7,77, 78, 79) increases with the presence of electron donating groups, provided desirable parameters such as degree of preorganization and conformation are not destroyed. This contributes to the stability of Gd<sup>3+</sup> complexes (82).

## 6 BASIC REQUIREMENTS FOR BIFUNCTIONAL CHELATORS AND COMPLEX FORMATION

A Bifunctional chelator usually consists of 3 parts: the binding unit, the ligand framework, and the conjugating group. The bifunctional chelate metal-complex must have a high thermodynamic and kinetic stability at neutral pH in order to keep the metal complex intact under physiological conditions and avoid toxicity from dissociation. The metal complex formed must have minimal number of isomers. Improved blood clearance and renal excretion is achieved with highly hydrophilic complexes. The conjugating group should easily bind to biomolecules (13).

Complexes are usually conjugated to macromolecules to target specific tissues, lesions, and cells. The chelate is usually conjugated via amide or ester linkages by simply mixing a readily available dianhydride form of the chelate with the macromolecule. However, formation of mono- and di-conjugated polyamine chelates would result in reduced affinities for the metal ion, leading to an increased number of inner sphere water molecules and greater toxicity. However, this does not happen because the weakly bound carbonyl oxygens of the amides and esters interact well enough to prevent both the dissociation of the complex and the entrance of additional water molecules into inner sphere of the  $Gd^{3+}$  complex (55). The problem of forming multiple carboxamides from DOTA, DTPA, and other polyaminocarboxylate agents is overcome by protecting the carboxylate groups in the form of activated esters of good leaving groups. For example, the three carboxylates of DOTA can be protected in the form of compound **1**, tris (tert-butyl) ester, or

compound **2** tris(phenylmethyl) ester (see figure 2). The main advantage of the latter derivative over the former is that the latter is easily coupled to a variety of carriers bearing amino groups. It also requires mildly acidic to neutral conditions for deprotection to the DOTA monoamide form, while the former requires more strongly acidic conditions (22).

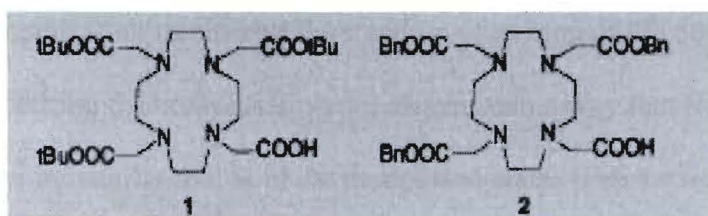


**Figure 2.** Protected derivatives of DOTA

## DENTICITY REQUIREMENTS

Denticity depends on the size and coordination geometry of the metal ion.

The large size of lanthanides (such as gadolinium) favors high coordination numbers (7, 8 to 9 donor atoms) to complete the coordination sphere and form stable complexes with macrocyclic chelators, such as DOTA and its derivatives, in aqueous media.

Chelators for lanthanide MRI contrast agents are mostly hepta-, octa- or nonadentate with at least one site open for water ligand exchange to enhance the water proton relaxation rates. All  $\text{Gd}^{3+}$  based chelates approved for use in MRI are nine-coordinate complexes in which a ligand occupies 8 binding sites at metal center and ninth coordination site is occupied by a solvent water molecule for proton relaxation .

In contrast, radiopharmaceuticals require higher denticity to provide enhanced thermodynamic stability and improved kinetic inertness (13), since they do not depend on water protons for imaging.

## LIGAND FRAMEWORK

Ligand framework refers to the spatial arrangement of the bonding units of the uncomplexed chelate. Polydentate ligands with 3-dimensional cavities can adopt a preorganized conformation in uncomplexed form. A high degree of preorganization of uncomplexed ligand increases stability and kinetic inertness of the complex. Preorganization minimizes the freedom of motion of the donor atoms and ligand framework during the complexation process in such a way that free ligand has a conformation more similar to that in the complexed state. The restricted freedom of motion minimizes the loss of entropy in forming the complex, leading to increased thermodynamic stability of the metal complex. For example,  $[\text{Gd}(\text{DOTA})]^-$  has half-life of 60.2 hours in 0.1M HCl while  $[\text{Gd}(\text{DTPA})]^{2-}$ , of similar thermodynamic stability, has  $t_{1/2} \sim 1\text{ min}$  (13).

The position by which the chelate is conjugated to a biomolecule can result in differences in stereochemistry and stability in three ways, as shown in Figure 3 (13).

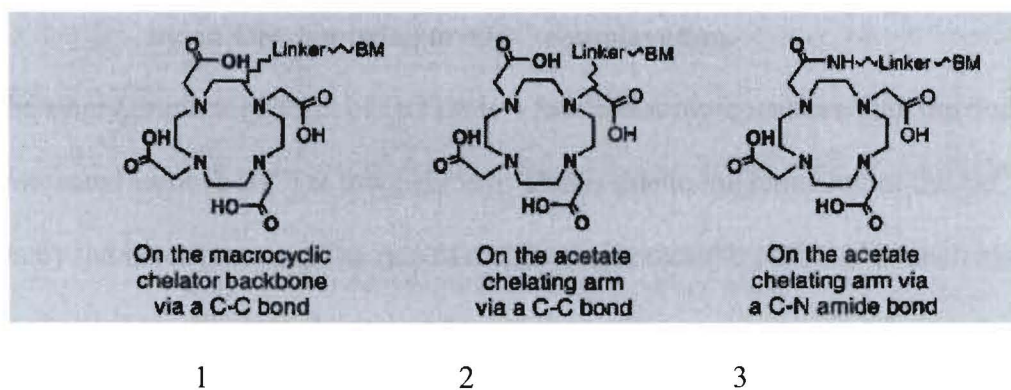


**Figure 3.** Different ways of conjugating macromolecules to DOTA ligand.

In cases 1 and 2, the conjugation with a biomolecule does not lead to a significant change in thermodynamic stability and kinetic inertness of the metal

complex relative to intact the DOTA –metal complex. However, conjugation of a biomolecule through an amide CO-NH bond formation with acetate group (case 3) lowers the thermodynamic stability of the metal due to the weak donor strength of the carbonyl oxygen compared to carboxylate oxygen. However, kinetic inertness remains unchanged, so the complex is highly stable in solution (13).

## METAL ION COMPLEXATION

DOTA forms stable complexes with several di- and trivalent metal ion complexes (3,56-58). In neutral solution, metal loading occurs in two steps as illustrated in Figure 4.

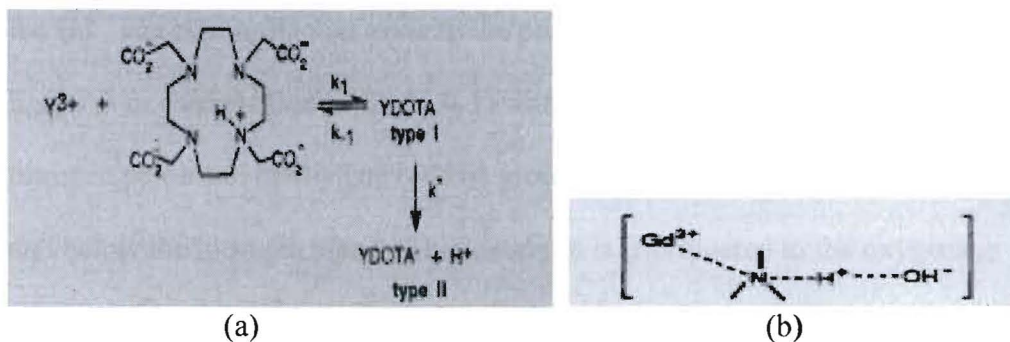


**Figure 4. Mechanism of a) metal ion ( $Y^{3+}$ ) complexation by singly protonated DOTA in neutral solutions and b) deprotonation of ligand nitrogen by an  $OH^-$  ion prior to  $Gd^{3+}$  complexation.**

The singly protonated form of DOTA is 4 four times more reactive than the doubly protonated form ( $LH_2^{2-}$ ) at low pH (59). This is due to the repulsion of the  $Gd^{3+}$  ion by the inner protons. The rate of metal complexation by DOTA is much higher at elevated temperatures because of rapid changes in conformation between the two isomers,  $LH^{3-}$  and  $LH_2^{2-}$  (60, 61). The carboxyl groups, amines, and the solvent water molecules on protonated DOTA are close enough to form hydrogen bonds with the protonated nitrogen. This facilitates deprotonation during metal

loading (56). Only the bio-conjugated, singly protonated form is more efficient in metal loading. Metal loading is usually 95% at room temperature in approximately one hour, even though conjugated DOTA has a lower metal loading. Metal loading is greater at high temperature ( $> 40^{\circ}\text{C}$ ) and at high pH (63, 64). Metal loading is faster in DOTA than in bio-conjugated DOTA because the amide carbonyl is less effective at hydrogen bonding than the carboxyl groups (84).

The stability constant of the  $\text{Gd}^{3+}$ -EDTA complex (98) is  $10^{9.81}$ (67).

If a nitrogen is protonated, electrostatic repulsion between  $\text{Gd}^{3+}$  and protonated nitrogen inhibits coordination of  $\text{Gd}^{3+}$ . Thus, in the intermediate form  $\text{Gd}(*\text{HL})$ , the  $\text{Gd}^{3+}$  ion is coordinated *trans* to the protonated nitrogen. The preorganized ligand is in conformation of (3, 3, 3, 3) with carboxylate oxygen on one side of the nitrogen plane and methylene ( $-\text{CH}_2$ ) groups alternating around the ring above and below the nitrogen plane. The metal ion is coordinated to the oxygens in the oxygen plane and at least one nitrogen the complex (69, 65).

The rate of metal complexation is faster for linear ligands than for macrocyclic polyamino carboxylate ligands (61,62,66,86). Reactions with more flexible ligands do not show the protonated intermediates, due to their fast reorganization. Thus, the macrocyclic polyamino carboxylates ligands are so rigid that their reorganization is slow, which retards deprotonation and exposes the protonated intermediate (65). The deprotonation process is assisted by the presence of  $\text{OH}^-$  ion. The proton is transferred from a protonated amine to the ( $\text{OH}^-$ ) hydroxyl. However, proton transfer to free water molecules is very unlikely, due to the highly unfavorable  $\Delta\text{pK}_a$  associated with the process. The deprotonation mechanism

is a highly concerted process in which  $Gd^{3+}$  ion moves into the vicinity of the nitrogen and the proton departs (65) to the hydroxyl ion simultaneously (see Figure 4b).

The structure of the preorganized ligand is such that the nitrogen lone pair or attached proton is directed inside the cavity of the macrocycle. However, metal complexation probably involves inversion of the nitrogen upon binding with the metal in the rate determining step. The energy required for rearrangement is proportional to the ligand strain energy (69, 70-72). Therefore, complexation is possible.

### **CONJUGATED GROUPS**

MRI ligands are conjugated to biomolecules to enhance targeting and relaxivity. This occurs through condensation via amide formation with active functional groups in the chelate. Ligands can be derivatized with active functional groups in the form of disulfide, diazobenzene, acid chloride or anhydride, N-hydroxysuccinamide (NHS) ester, aldehydes, and ketones (13,134). The biomolecules may be proteins, DNA, or other biologically active molecules. NHS-activated ester is mildly reactive towards amines, and has a high selectivity for aliphatic amines. The optimum pH for carrying out such a reaction in aqueous systems is 8 to 9. Virtually any molecule containing a carboxylic groups can be converted to its NHS ester, making NHS-activated ester groups one of the most powerful and most commonly used agents for conjugating or attaching molecules to chelate complexes. Water soluble NHS-activated ester is often used to conjugate biomolecules to DOTA (13).

## CHOICE OF BUFFER

The choice of buffer depends on the optimum pH value for complexation. Use of phosphates and carbonate /bicarbonate buffers should be avoided, especially for acyclic chelates, since both phosphates and carbonate readily form precipitates with the lanthanide ions. DOTA forms zwitterions in solution with the conformation determined by the degree of protonation. For example, at pH 3.6 to 5, the predominant form is  $H_3 [(DOTA)]^-$ , while it exists primarily (90%) as  $H_2[(DOTA)]^{2-}$  at pH 6 to 7 (136,137).

## 7 APPLICATIONS

Total tissue water comprises Intravascular (5%), Interstitial (fluid space between cells and capillaries) (15%) and Intracellular space (80%). The intracellular component is divided by cellular organelles. A decrease in effective tissue relaxation of an agent might occur if water exchange between any of the compartments is slow relative to the relaxation rate in compartments with the longest  $T_1$ , because not all tissue water is encountering paramagnetic centers.

When administered intravenously, the chelate rapidly equilibrates in extracellular fluid compartments in the intravascular and interstitial spaces. Agents may also pass into cells (including liver and kidney cells) by passive diffusion or specific uptake processes. Small molecular mass hydrophilic chelates that do not bind to plasma proteins are non-specifically filtered out by the kidneys (glomerular-filtration) and excreted in the urine. MRI agents containing aromatic rings are partly hydrophobic and some are taken up by liver cells and excreted into bile (hepatobiliary excretion). These molecules can also bind to plasma protein (such as albumen), reducing the free fraction available for glomerular filtration. This slows the renal excretion rate and prolongs blood half-life and imaging time (1).

### RENAL EXTRACELLULAR AGENTS

These have dominant use as MRI agents. (110,111,112). They distribute non-specifically through the plasma and interstitial spaces of the body after injection and are excreted by the kidneys with an elimination half-life of 1.5 hours.

$[\text{Gd}(\text{DOTA})(\text{H}_2\text{O})]^-$  is a renal non-specific agent or non-selective extracellular agent (that is, localization in tissue is not determined by specific cellular process).

The carboxylate and other charged or hydrogen-bonding groups minimize interactions with plasma proteins, other macromolecules, and membranes. The distribution

of the complex equilibrates in extracellular space and is removed by renal excretion. This application utilizes bulk tissue  $1/T_1$  dependence on volume distribution for the agent (20, 21,138). If water exchange between extracellular and intracellular compartment is fast relative to their  $T_1$ 's, then bulk tissue  $1/T_1$  before injection of the agent is:  $(1/T_1)_{\text{pre-inj}} = f_{\text{ex}} (1/T_1)_{\text{ex,pre}} + f_{\text{in}}(1/T_1)_{\text{in}}$  where  $f_{\text{ex}}$  is fraction of water protons in extracellular space. The term  $[1/T_1]_{\text{exp,pre}}$  represents the extracellular relaxation rate in the absence of paramagnetic species,  $f_{\text{in}}$ , and the intracellular fraction is characterized by  $[1/T_1]_{\text{in}}$ . Extracellularly localized agents increase  $[1/T_1]_{\text{ex}}$  directly:

$$\begin{aligned} \text{Net change in overall tissue } 1/T_1 \text{ is } [\Delta(1/T_1)] &= [1/T_1]_{\text{post,inj}} - [1/T_1]_{\text{pre,inj}} \cdot \\ &= f_{\text{ex}}[1/T_1]_{\text{ex,post}} + f_{\text{in}}[1/T_1]_{\text{in}} - f_{\text{ex}}[1/T_1]_{\text{ex,pre}} - f_{\text{in}}[1/T_1]_{\text{in}} \\ &= f_{\text{ex}}[(1/T_1)_{\text{ex,post}} - (1/T_1)_{\text{ex,pre}}] \end{aligned}$$

Tissues have the greatest signal intensity changes if the MRI agent equilibrates to roughly the same concentration in extracellular space where  $(1/T_1)_{\text{ex,post}}$  is relatively constant in different tissues. This occurs in tumors and abscesses where there is often increased interstitial volume (116,117,118).

This is applied in fast imaging of kidneys, and in structural and functional blood flow to tissue (perfusion) (114,115), fast imaging of arteries and blood flow to the heart, fast imaging detection of cerebral capillary breakdown, brain tumor detection and imaging, enhancement of tissues having increased extracellular volume, etc.

In detection of brain lesions, normal tissues show little enhancement because of the impermeable nature of blood capillaries in the brain (blood brain barrier) and the small intravascular volume distribution (~5%) of the agent gives little enhancement to normal brain tissues. However, capillaries in the tumor area are permeable,

causing blood filtration. The complex then passes into the interstitial space, leading to selective MRI enhancement of the tumor (119).

## **HEPATOBIILIARY AGENTS**

Uptake of these agents into liver cells seem to be mediated by specific receptor proteins or carrier transport agents. The uptake of these agents is similar to the uptake of bilirubin or fatty acids, and dyes, since they are structurally similar. These molecules are extracted, even though they bind to blood albumin, therefore, some diffusion into hepatocytes may occur at the cell surface. The presence of hydrophobic and hydrophilic groups in high molecular weight compounds (>300 for RATS and >500 for humans) direct the MRI agents to the bile in preference to urine. The lipophilic groups (such as aromatic groups) interact favorably with the hydrophobic parts of membrane receptors or other transport proteins (113). The greater lipophilicity (hydrocarbon chain or aromatic rings) gives greater hepatobiliary excretion. High lipophilicity leads to localization of the agent into fat storage sites or membrane fat receptors. The lipophilic agent might form aggregates, precipitate in the aqueous environment of the blood, and then be removed by reticuloendothelial cells in the liver and spleen, resulting in chronic toxicity due to long term retention. Targeting of low concentration (<1mM) receptor sites is not possible for MRI, due to the high concentration of paramagnetic agents needed for image enhancement compared with other methods. Hydrophobic groups (such as hydrocarbon groups) on chelates lead to hepatobiliary uptake and excretion into bile ducts, gall bladder, and intestines. High lipophilicity slows the motion of the complex, leading to increased relaxivity.

A lipophilic gadolinium complex has been synthesized and formulated as mixed micelles (see figure 4) to enhance uptake by the hepatobiliary cells of the liver.

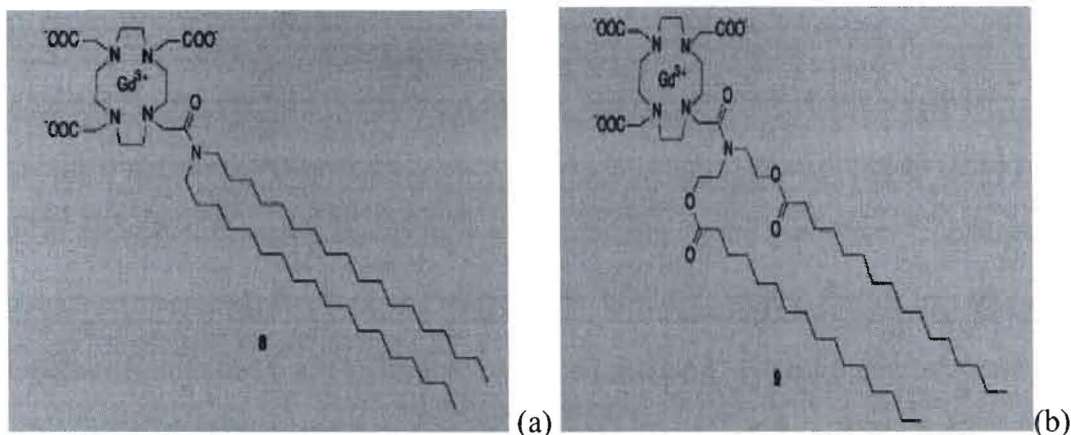


### Figure 5. Gd-DOTA lipophilic agents with long hydrocarbon esters

Compound **8** (Figure 5a) in mixed micelles (multicompatible non-ionic surfactant mixed with lipophilic gadolinium complex) has been synthesized for magnetic resonance imaging. This gave high relaxivities and long blood residence time in rats. However, there was poor elimination. Seven days after injection in rats, only 50% of **8** was eliminated by the liver while the rest remained in the animals body. However compound **9** (Figure 5b) was more easily eliminated due to presence of the two palmitic ester groups. These are easily hydrolyzed *in vivo* to produce a small hydrophilic gadolinium complex that is easily eliminated. Seven days after injection in rats, 67% of **9** was eliminated and 7% of the injected dose was found in urine. This provides indirect evidence of partial hydrolysis *in vivo* (22). Thus, hepatobiliary agents can be used in the imaging of the liver, bile duct, intestines, and gall bladder. Possible diagnostic applications include detection of small lesions such as metastatic tumors (focal liver disease) and diffused liver disease (such as liver cirrhosis), by imaging of the bile ducts and the gall bladder (1).

## BLOOD POOL AGENTS

Blood pool agents are lipophilic agents that are targeted to bind to blood proteins such as human serum albumen (HSA) or bovine serum albumen (BSA) for imaging blood vessels in the body and examining blood perfusion. The large molecular mass, together with the high protein binding affinity, results in a longer residence time in the body and improved blood imaging. High lipophilicity and greater protein binding affinity slows the motion of the complex, leading to increased relaxivity (101,139).

Trapping of paramagnetic agents in intravascular spaces, either because of to molecular size or binding to plasma proteins, would enable enhancement of normal, perfused tissues relative to infarcted tissues (tissues with decreased blood supply). This can enhance smaller blood vessels as well. These agents are either paramagnetically labeled proteins or polymers of greater than 60,000 molecular weight. HSA can also be used for small molecule weight chelates that bind strongly (1,101).

Preparation and characterization of the gadolinium complexes of poly-L-lysine Poly-(diethylenetriamine-N,N',N'',N'''-pentaacetic acid), Gd-PL-DTPA (Figure 6a), poly-L-lysine–poly(1,4,7,10-tetraazacyclododecane–N,N',N'',N'''-tetraacetic acid), Gd-PL-DOTA (Figure 6b), and their conjugates with Human Serum Albumin (HSA) (Figure 6c) has been carried out (17). N-acylation of poly-L-lysine with a mixed anhydride of the chelating ligand DTPA or DOTA allowed 60 to 90 chelating groups to be attached to each molecule of polylysine and HSA. This resulted in 2-3 fold increased molar relaxivities compared to the monomeric complexes [Gd(DTPA)] and [Gd(DOTA)] (12).

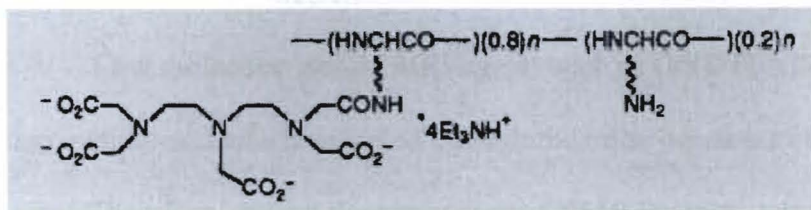


Figure 6a. Structure of PL-DTPA

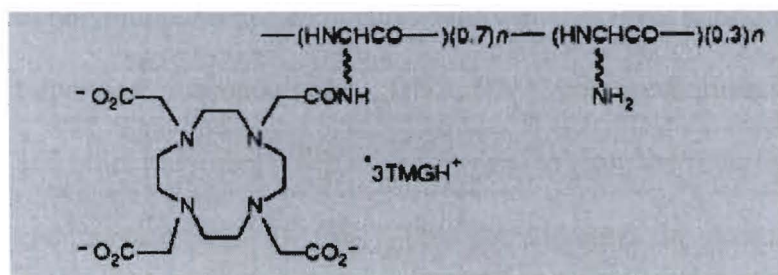


Figure 6b. Structure of PL-DOTA

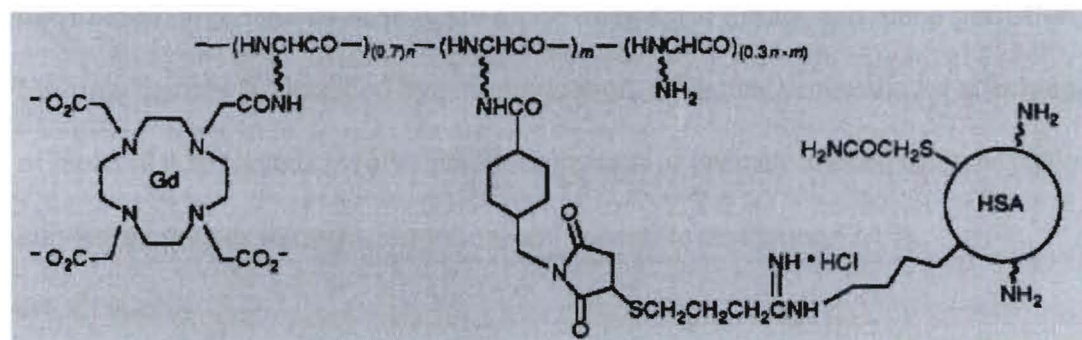


Figure 6c. Structure of PL-Gd(III)DOTA conjugated to HSA

## 8 MACROMOLECULAR CONJUGATES

Low molecular weight MRI agents such as  $\text{Gd}(\text{DTPA})^{2-}$  and  $\text{Gd}(\text{DOTA})^-$  are rapidly and totally excreted through the urine because of their small molecular size. Therefore, several doses are needed NMR imaging, which in prolonged clinical tests, increases *in vivo* toxicity (92). The problem can be avoided by conjugating to polymers or macromolecules such as monoclonal antibodies (134,135) proteins (albumins, immunoglobins), DNA, RNA, polysaccharides (93), dextrans (1), dendrimers, and other polymers (such as polylysine) to slow the rotational speed of the MRI agent and increase relaxivity (101). This also increases the plasma persistence and plasma half-life which can be used in blood pool tracers (95).

High molecular weight conjugates, which are retained in vascular tissues due to their large molecular size, aid blood imaging of tissues and blood perfusion. Multiple ligands are attached by polymerization. Chemical processes for attaching of molecules to ligands involve functionalization of primary amines using acylation, alkylation, urea or thiourea formation, and reductive amination (2,13).

### DEXTRANS

Polydextrans can be used to hold several chelates, due to the availability of many attachment points. They occur in different molecular weights. They have high solubility in the plasma, which makes them useful as plasma volume expanders (2) and also potential transfer agents for solubilizing MRI agents. Binding to cyclodextrins slows the molecular tumbling time ( $\tau_R$ ) and increases relaxivity. A Gadolinium–DTPA complex conjugated to dextrans (see Figure 6a) has been synthesized for MRI. This MRI agent has good paramagnetic properties and long

intravascular persistence, biocompatibility, and biodegradability. The partially cross-linked polymer with reduced complexation capacity was found to have 2.5 times higher relaxivity than free GdDTPA<sup>2-</sup> (11). The large molecular mass increases plasma half life relative to the free ligand or dextran polymer. Also, due to the high relaxivity per mole of Gd, a lower concentration of the conjugate is needed to obtain a contrast than with the free ligand complex (92).

Increasing the length of the methylene chain spacer arms (29) does not affect relaxivity, however, it reduces toxicity of the contrast agent because of the increased molecular mass (96). This shows that even though conjugation to macromolecule reduces the tumbling and thus the rotational correlation time, it is unnecessary to lengthen polymer chains because electron spin relaxational time and water proton exchange relaxation time are sufficiently short and this limits any additional increase in overall relaxational correlation time (94).

Another similar agent that has been synthesized for MRI is a Gd(DOTA) complex conjugated to Gd(DOTA) complex conjugated to  $\beta$ -cyclodextrans (Figure 7b). Relaxivity of these modified CMD polymers ranges from 6-11 mM<sup>-1</sup>s<sup>-1</sup> at 37°C at 20MHz (8,10, 32, 33).

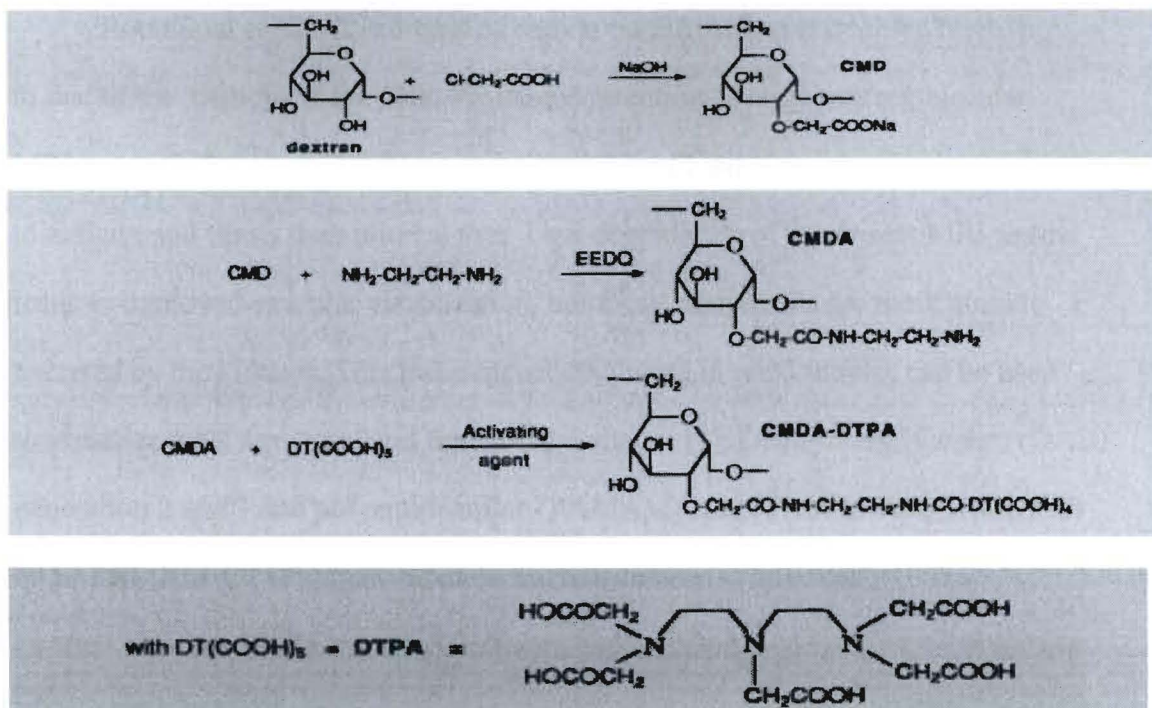


Figure 7a. Synthesis of CMDA-DTPA [(EEDQ = 2-ethoxy-1-(ethoxycarbonyl)-1,2-Dihydroquinoline)]

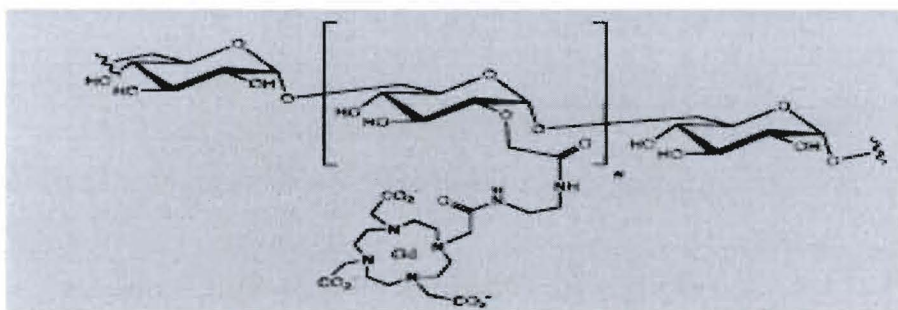
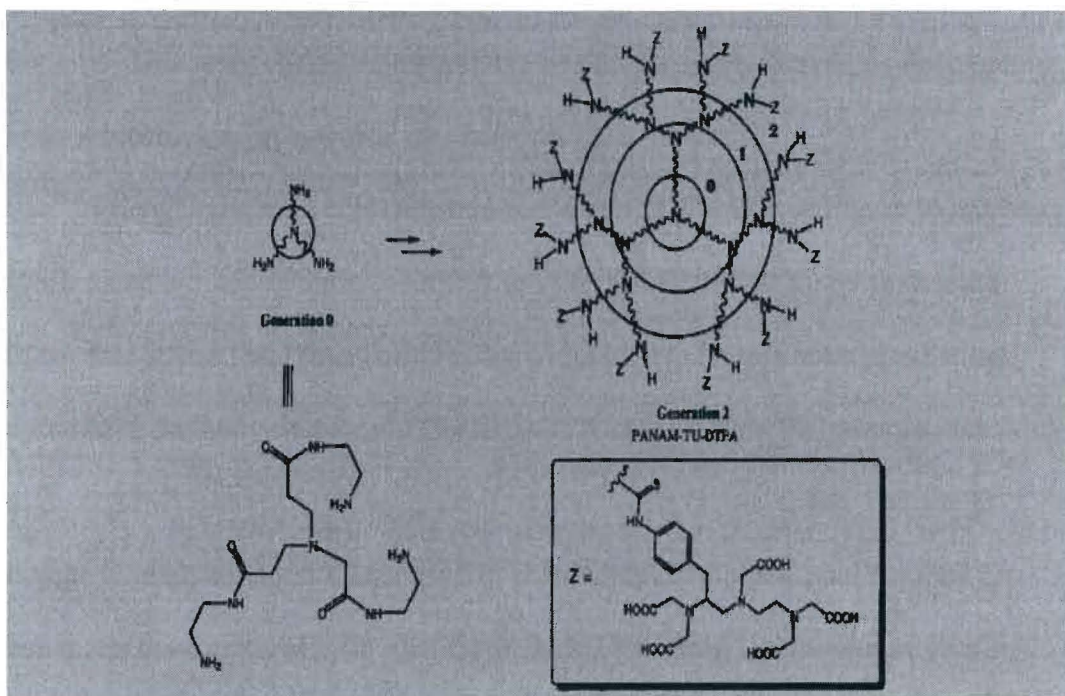


Figure 7b. Macrocytic CMD-A2-Gd-DOTA

## DENDRIMERS

Dendrimers are 3-dimensional, oligomeric structures made by repeated reaction sequences starting from a smaller core. Gd(III) chelate dendrimer conjugates have uniform surface chemistry, reduced molecular weight distribution, and shape variations. Their rigid structures, together with the overall tumbling of the molecules, contribute to their increased rotational correlational time.

Rotational correlational time of carbon on the surface is doubled relative to that of the carbons at the core. Prolonged retention of large macromolecular MRI agents (albumin or dendrimer cores) used for blood vessel imaging contributes to toxicity and limits their clinical use. Less degradation of dendrimer MRI agents leads to improved vascular visualization, but these compounds are more quickly excreted by the kidneys. This transient accumulation in renal tubules can be used to visualize renal structural and functional damages (1). Dendrimers Diamino (DAB) generation 2 and 3 and polyamidoamine (PAMAM) core [PAMAMG4-(IB4M-Gd) 64 or PAMAM-G4 (Figure 8) used on mice have been synthesized (100).



**Figure 8.** Generation-2-PAMAM thiourea dendrimer .

If rapid rotation of the attached chelate is the limiting factor, then there should be an increase in relaxivity by conjugating MRI agents to dendrimers.

Unlike dendrimers, linear polymers have slow water exchange, which limits relaxivity ( $\tau_m$ ). Rigid dendrimeric structures result in fewer degrees of freedom for

conjugated gadolinium chelates, along with high  $\tau_R$  and high relaxivity. For example, Gd-DOTA chelate conjugated to PAMMAM starburst dendrimer has the largest number of Gd(III) ions per macromolecule (142,143).

## BIOMOLECULES

Proteins, polysaccharides, and nucleic acids monoclonal antibodies (19,23,24) are naturally occurring polymers that are often conjugated to MRI agents. For example, human serum albumin or bovine serum albumen conjugated to Gd-DTPA is used as the “gold standard” for blood pool agents (2,13). Slow excretion results in the metabolism of macromolecular Gd<sup>3+</sup> complexes and release the of Gd<sup>3+</sup> ions, causing toxicity. This is solved by using conjugates that are easily cleaved by endogenous body molecules, which speeds up excretion from the body.

Poly-(L-glutamic acid)–cystamine–[Gd(III)DOTA] (see Figure 9) has been synthesized by conjugation of DOTA to PGA (M.W. = 50000) by cystamine (cleavable spacer) and then complexing with GdCl<sub>3</sub>. Endogenous plasma thiol cysteine in the body will cleave Gd(III)DOTA chelate from the polymer, resulting in excretion of the complex by renal filtration. Tests on male mice bearing OVCAR-3 human ovarian carcinoma xenographs, shows impaired blood pool contrast enhancement compared with that from Gd(DTPA-BMA), a smaller molecule (25).

The macromolecules remain intact during the imaging process while Gd(III) chelate complex is released from the polymer by endogenous biomolecules that cleave the spacer. Excretion of the agent is controlled by injecting exogenous substances after imaging (25). The Gd(III) complex is an extracellular agent and the low concentration of thiol in the plasma (15 $\mu$ M) will slow the rate of cleavage

of the disulfide spacer and excretion of agent, allowing an acceptable time window for effective diagnostic imaging. However, cleavage rate and excretion of the Gd(III) agent can be accelerated by administering exogenous thiols after MRI exams (25).

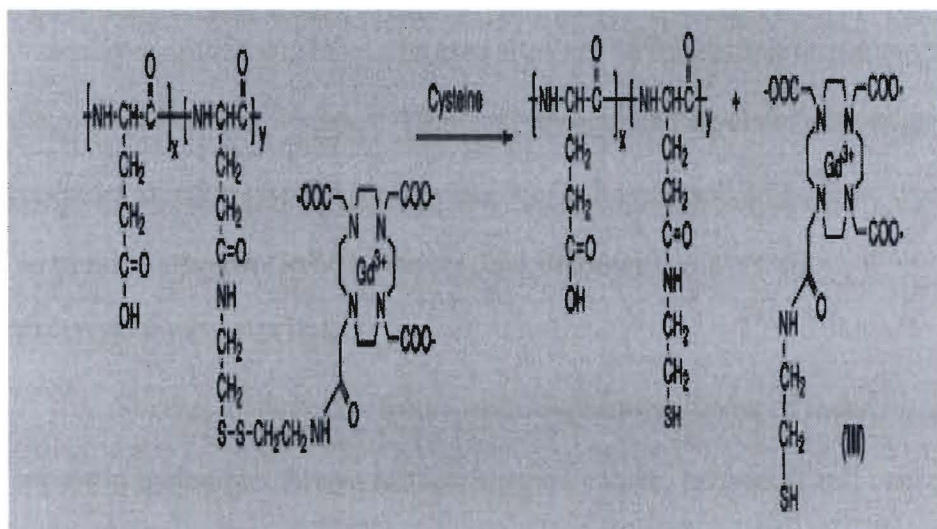


Figure 9. Poly(L-glutamic acid)–cystamine–[Gd(III)DOTA]

## 9 TUMOR TARGETING

Tumor targeting relies on the fact that certain body receptors are over-expressed in diseased tissues, but are limited in normal tissues. Receptors on vascular endothelial cells at diseased sites are an interesting target and simplify diagnosis of several diseases. High and upregulated levels of activation-related receptors are expressed in blood vessels of inflamed and angiogenic tissues such as tumors, atherosclerotic plaques, and rheumatic joints (36).

### TUMOR RECEPTORS

Several different receptors occur in tumors. Some of these,  $\sigma$ -receptors, appear in melanoma, breast cancer, prostate cancer, and small cell cancer of the lungs (30). Their function is not very well known. There are also receptors for peptides and other small molecules that are overexpressed in breast cancer and other tumors. Some of these receptors include G-protein-coupled receptors, type-2 somatostatin receptors, tyrosine kinase receptors, (such as vasoendothelial growth factor receptor (VEGF-R)), insulin receptors, insulin-like growth factor type-1 receptor, epidermal growth factor receptor (EGF-R), fibroblast growth factor receptor (types 4 and 1) nontyrosine kinase receptor, and the  $\beta$ -subunit for the interleukin-2 receptor (30).

### FOLIC ACID RECEPTORS

Cell accumulation of folic acid (FA) and its derivatives is mediated by membrane cell surface folic acid receptors. Occurrence of these receptors is limited in normal tissues but widespread in certain tumor cells especially ovarian carcinomas, breast cancers, epithelial cancers, colorectal, lung, renal, and brain metastases (30, 44, 48).

Limited distribution of folic acid receptors occur in normal human tissues, mainly in the kidneys, lungs, choroid plexus, and placenta. The receptor in each of these tissues (except placenta) are localized in the apical membrane and thus are not accessible to FA conjugates administered intravenously (44,48).

### **QUALITIES OF A GOOD FOLATED AGENT**

Some unique properties of folic acid that make it suitable for targeting receptors include the following:

- a) It has a low molecular weight, so it is quickly filtered off by the kidneys.
- b) High affinity folic acid receptors are greatly enriched in cancer or tumor cells
- c) It allows targeting of agents to neoplastic tissues.
- d) It easily conjugates to PEG through amide or peptide linkage
- e) There is no allergic immune response to the use of folate agents.
- f) Folate mediates endocytosis of agents into non-lysosomal compartments.
- g) Folate ligand is inexpensive, stable during storage and *in vivo* circulation, intrinsically nontoxic, and easy to conjugate to desired agents (39).

### **USE OF POLYETHYLENE GLYCOL (PEG) LINKER AND ITS LIMITATIONS**

Conjugated target agents or surface modified agents are susceptible to agglomeration due to large or increased surface-to-volume ratios. Agglomerated agents lose their functionality and are also quickly cleared by macrophages of the reticuloendothelial system or mononuclear phagocyte system (liver and spleen) before they can reach target cells. The problem is solved by use of a PEG linker in the agent. PEG attached to liposomal bilayer builds up a sterically repulsive shield that protects the liposomal surface to prevent aggregation, agglomeration, and nonspecific binding to plasma proteins. Thus, they interfere with liposomal recognition

and clearance from circulation by the macrophages of the reticuloendothelial system. PEG-coated agents are nonimmunogenic, nonantigenic, and protein resistant (40). They have long circulation times, leading to increased localization in tumor tissues with high microvascular permeability (42). However, the increased molecular weight reduces the cell uptake and biological activity of the drug (31,53), which resides mostly in the extracellular medium.

Liposomal formulation containing distearoylphosphatidylethanolamine (DSPE) linked with PEG to a biological cell adhesive YIGSR peptide or Sialyl Lewis x oligosaccharide (Figure 10) was synthesized for *in vivo* drug delivery studies with long circulating liposomes (44,46). Increase in folate receptor binding was observed with increased molecular mass of the PEG tether from 200-3350 Da, especially when binding inhibitor mPEG (methoxy-PEG) is present.

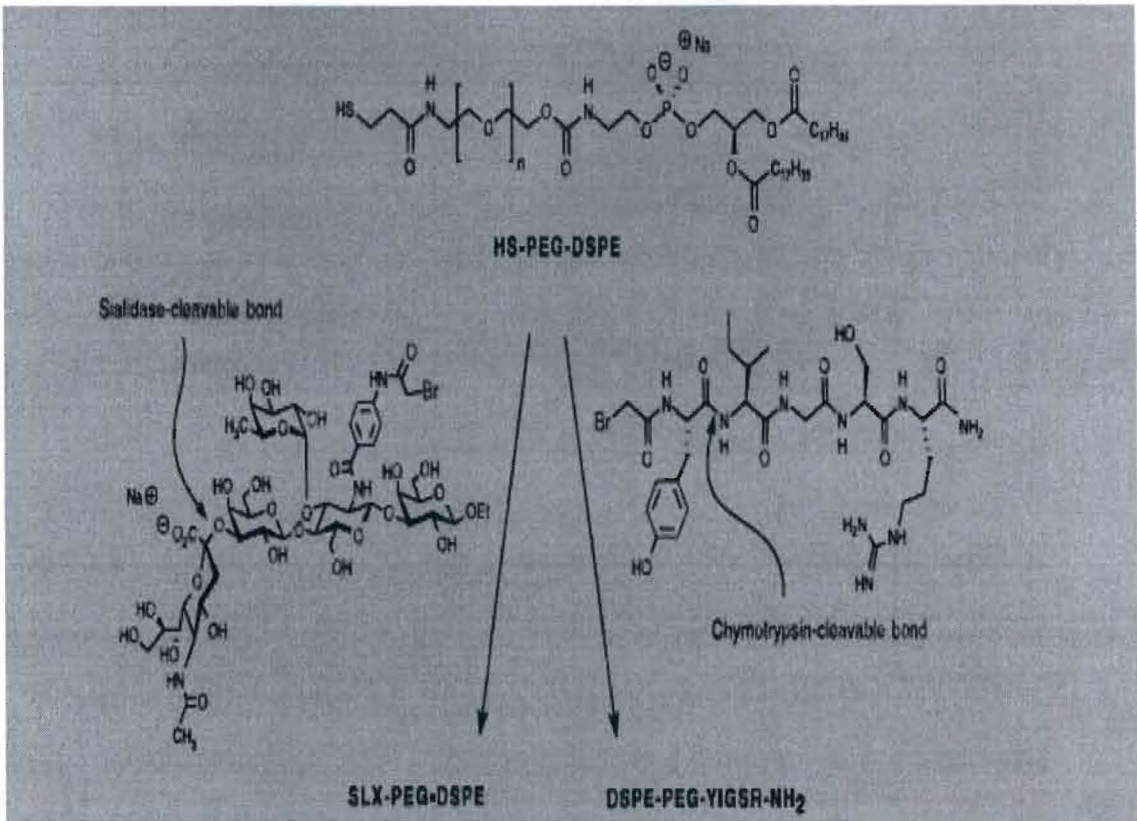


**Figure 10.** HS-distearoylphosphatidylethanolamine (DSPE) liposomal agent linked with PEG.

High expression of E-selectin /CD62E adhesion molecular markers was induced by treatment of human umbilical vein endothelial cells (HUVEC) with pro-inflammatory cytokine tumor necrosis factor  $\alpha$  ( $\alpha$  TNF $\alpha$ ). E-selectin is a molecule involved in leukocyte vessel wall interactions and is highly upregulated in inflammatory cytokines (36).

Incubation of E-selectin expressing HUVEC with anti-E-selectin targeting ligand conjugated to pegylated paramagnetic fluorescently labeled liposomes (see figure 11) reveal their specific points of contact. Thus, this can be used for imaging diagnosis. E-selectin binds to E-selectin molecular markers in HUVEC and are internalized by these cells (36).

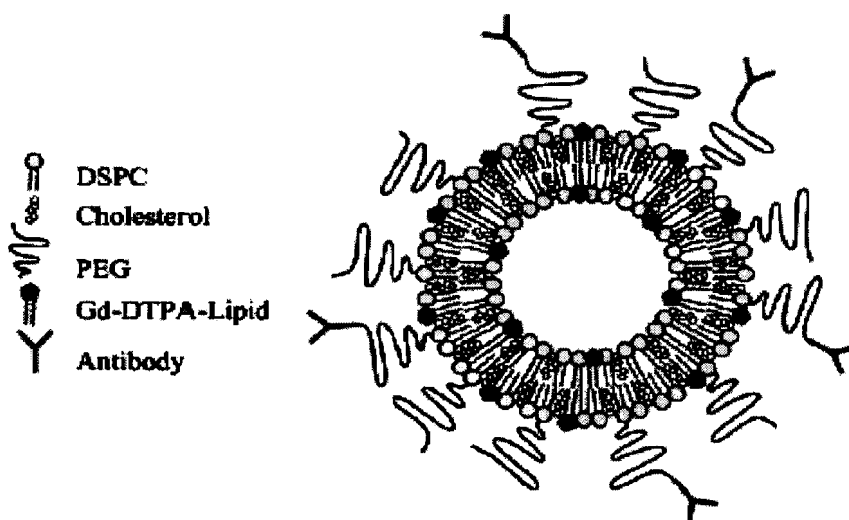


**Figure 11.** Liposomal Gd-DTPA agent conjugated to E-selectin antibodies for targeting HUVEC

### MECHANISM OF FOLATE RECEPTOR MEDIATED ENDOCYTOSIS

Folic receptor (FR) is a glycosylphosphatidyl-inositol-linked membrane glycoprotein of 38 kDa located *in caveolar* that participates in the cellular accumulation of folates in a number of epithelial cells through the process of pinocytosis. In this process, ligand bound receptor is sequestered *in caveolar*, followed by internalization into postcaveolar plasma vesicles, released from the receptor through an intravesicular reduction in pH, and subsequently transported into the cytoplasm for polyglutamation. Reopening of the caveolae (34, 35, 38) then recycles the ligand free receptor. The folate targeted conjugates are not freely released into the cytosol but are directed to acidic cytoplasmic vesicles such as endosomes and lysosomes. Release of the agent may be slow and inefficient, thus reducing the cytotoxicity of the delivered complex (31,37). Folate-derivatized boronated liposomes have higher cellular uptake in human KB squamous epithelial cancer cells (see Figure 11) enriched with folate receptors expression than nontargeted control liposomes. This boron neutron capture therapy (BNCT) is currently under consideration to be used for therapy and diagnosis

of primary and metastatic brain tumors and cutaneous and metastatic melanoma (51).

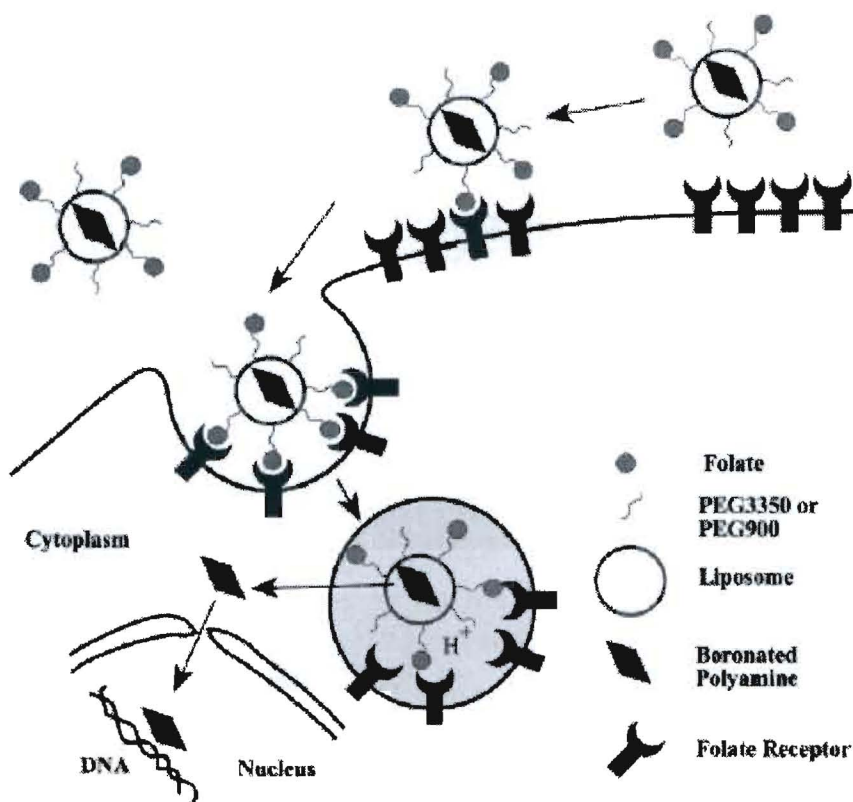


**Figure 12. Folate receptor endocytosis mechanism for delivery of boronated agents for intracellular targeting of DNA of tumor cells (51). Encapsulated boronated agent is then released into the cytosol via endosomal escape and bound to the DNA in the cell nucleus.**

#### **APPLICATIONS OF FOLATED AGENTS FOR TUMOR TARGETING**

Gd-157 hexanedione (GdH) (Figure 13a) complex was synthesized by complexation of  $Gd^{3+}$  with 2,4-hexanedione as a nanoparticle matrix or combined with either emulsifying wax or PEG-400 monostereate. A folate ligand was synthesized by chemically linking folic acid to distearoyl-phosphatidylethanolamine (DSPE) via poly(ethylene glycol) (PEG MW 3350) spacer (Figure 13b). The folate ligand was linked to the gadolinium complex (as microemulsion at 60°C or as nanoparticle at 25°C). Investigation of efficiency of cell uptake with KB cells (human nasopharyn-

geal epidermal carcinoma cell line) known to be enriched with folate receptors showed a 10-fold increase in cellular uptake of folated complex relative to unfolated complex at 37°C after 30 minutes. However, uptake at 4°C was 20 fold lower than at 37°C (37).

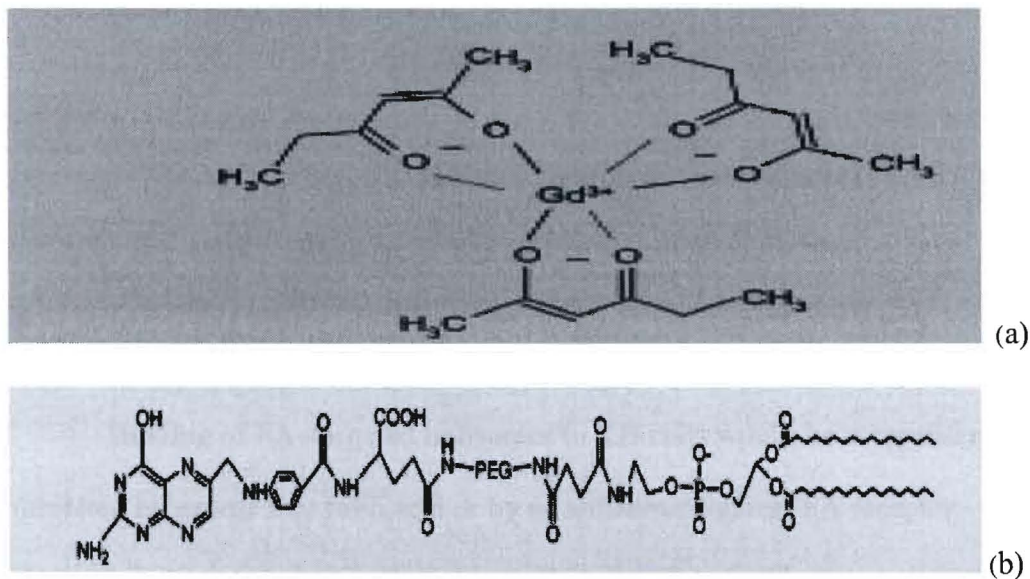


**Figure 13.** a) Gadolinium hexanedione (GdH) complex. b) Structure of folate-PEG-DSPE-synthesized by linking folic acid to DSPE via a PEG spacer (M.W. 3350).

Conjugates of folic acid-poly (ethylene glycol)-distearoylphosphatidyl-ethanol-amine (FA-PEG-DSPE), derived from PEG with molecular masses of 2000 and 3350 Da, were synthesized by a carbodiimide coupling of FA to H<sub>2</sub>N-PEG-DSPE (see Figure 14). This was used to significantly enhance liposome binding to tumor cells (44).

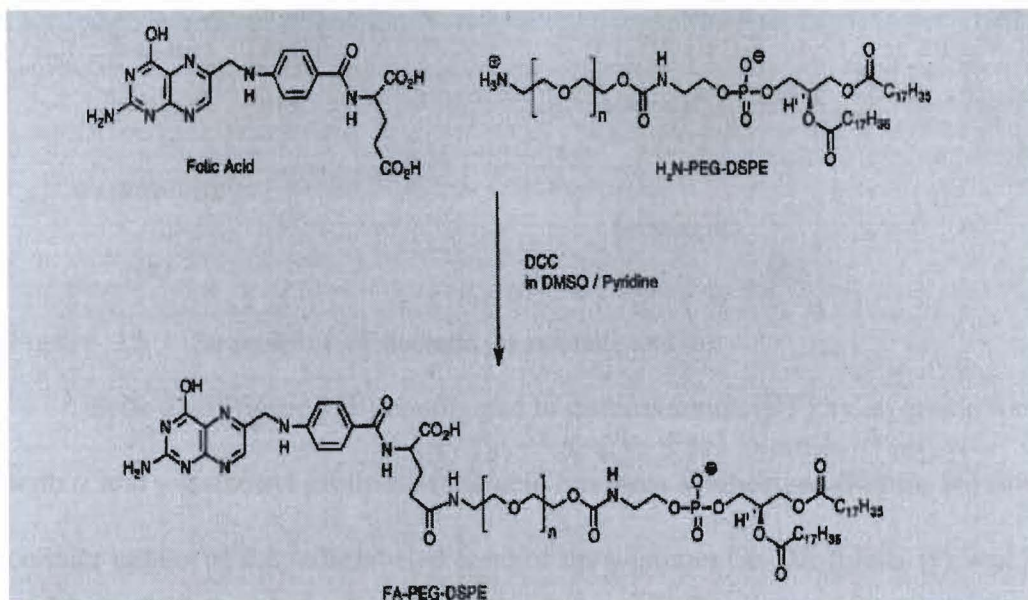


**Figure 14.** Synthesis of folic acid conjugated to DSPE via PEG spacer.

Binding of FA-targeted liposomes to KB cells would be competitively inhibited by excess free folic acid or by an antiserum against FA receptor. This shows that the process is mediated by cell surface FA-binding protein (44,47,48). Folic acid derivatized at the  $\alpha$ -carbonyl group has a high affinity for folate receptor ( $K_a \sim 10^{10} \text{ M}^{-1}$ ) (102).

Carboplatin (see Figure 15a), a platinum containing antitumor agent, has been conjugated to folate-targeted PEG carriers. FA-PEG-Pt and FA-PEG-FITC were synthesized and their cell uptake, DNA binding, and cytotoxicity were studied by fluorescent microscopy, FACS, and platinum analysis. It was found that cell uptake occurs efficiently by folate-receptor mediated endocytosis. However, DNA binding and cytotoxicity were lower compared to non-folated non-targeted PEG analogues (31).

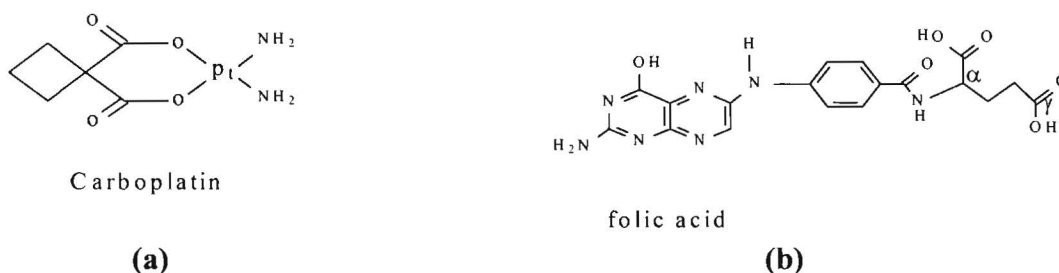


**Figure 15.** Structure of carboplatin (a) and folic acid (b).

Folic acid (figure 15b) conjugated to deferoxamine (DF) by an amide formation with  $\alpha$  and  $\gamma$ -carbonyl group on folic acid has been synthesized (Figure 16) (48). The cellular uptake of the radiolabeled form of the  $\gamma$ -isomer Ga-DF-folate- ( $\gamma$ ) was found to be folate receptor mediated and is time, temperature, and concentration dependent. Uptake half-life was found to be almost 3 minutes. This has a viable potential of being used for tumor detection (31,32,33).

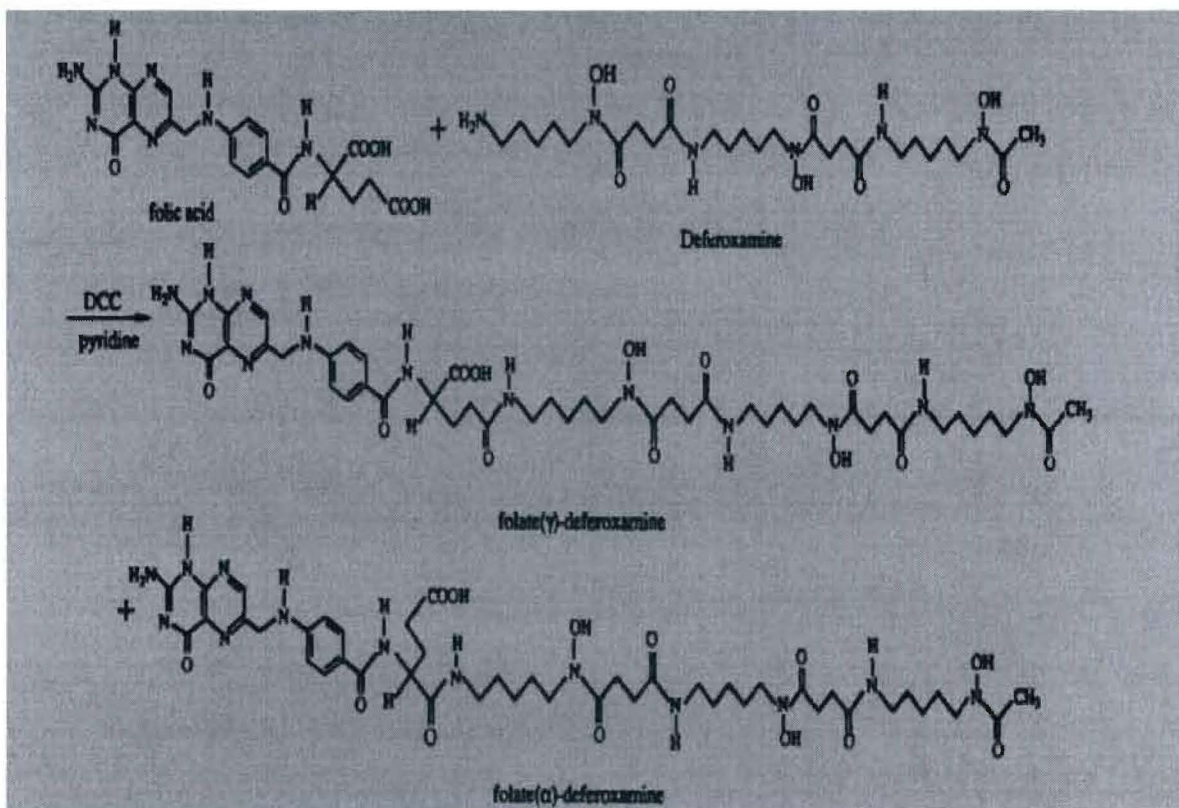


**Figure 16.** Synthesis of folic acid conjugated to deferoxamine.

It has been reported that when the folate group is covalently conjugated to the macromolecule through the  $\alpha$ -carboxylate moiety, its affinity for cell surface receptors remain essentially unaltered. This property has been successfully exploited to deliver folate-conjugated protein toxins and drug/antisense oligonucleotides carrying liposomes into cultured tumor cells overexpressing the folate receptor (44).

## 10 SOLID-PHASE OLIGONUCLEOTIDE SYNTHESIS

In the standard four-step phosphoramidite process (Figure 17), the 5'-*O*-dimethoxy trityl (DMT) group is removed from a deoxynucleoside linked to polymer support. Elongation of the growing chain oligodeoxynucleotide (ODN) occurs by the initial formation of a phosphite triester internucleotide bond. A capping agent is reacted to esterify failure sequences. The phosphite internucleotide linkage is oxidized to the corresponding phosphotriester. A large excess of trichloroacetic acid (TCA) in dichloromethane is used to remove DMT from the growing oligonucleotide. This process is repeated to generate an ODN of desired length and sequence. Treatment of the solid support with  $\text{NH}_4\text{OH}$  cleaves the ODN from the column and removes  $\beta$ -cyanoethylphosphate protecting groups (43).

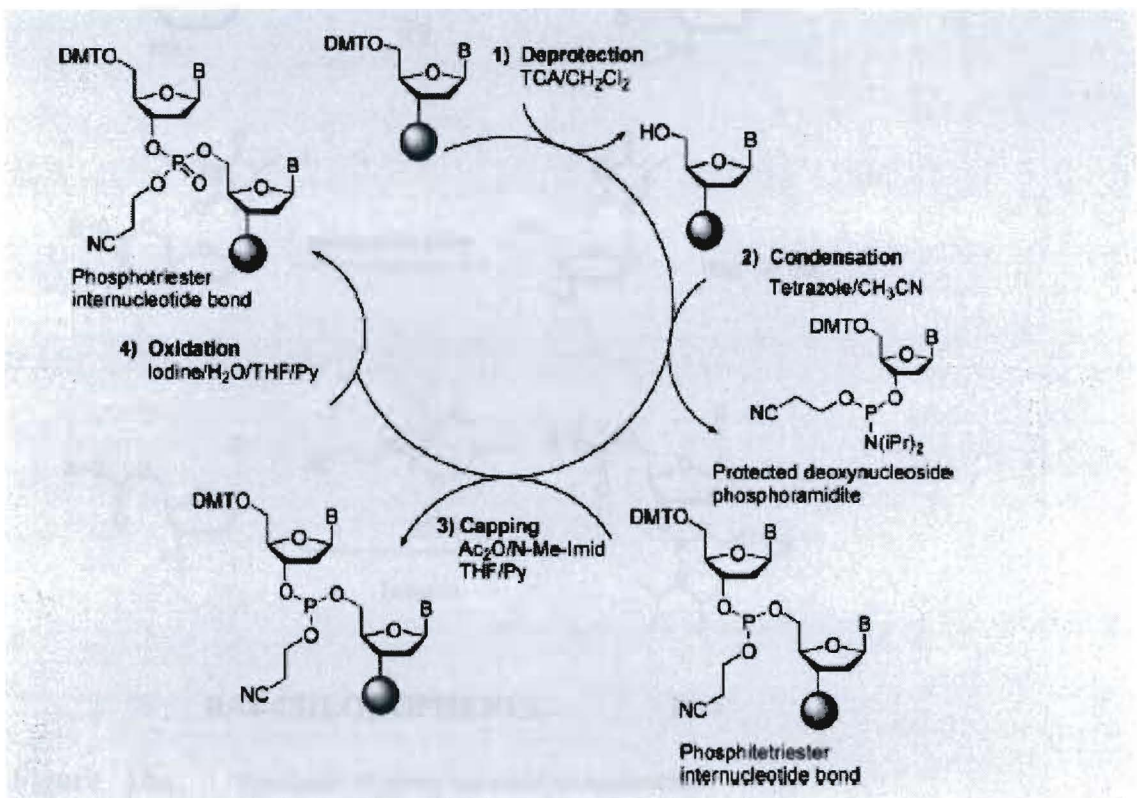


**Figure 17.** DNA synthesis by standard four step phosphoramidite process

This process has been used for about 20 years for most biological research, such as DNA sequencing, PCR, and site-specific mutagenesis. However, a new two-step approach to ODN synthesis has been developed (Figure 18b) in which the 5'-dimethoxytrityl blocking group was replaced with an aryloxy carbonyl, while the exocyclic amines were protected with N-dimethoxytrityl groups. An aqueous solution of peroxyanion, buffered at pH 9.6, is used to monitor the coupling of each 2'-deoxynucleoside-3'-phosphoramidite (Figure 18a) to the growing oligodeoxynucleotide on the solid support. This removes the carbonate protecting groups and oxidizes the phosphite to phosphate internucleotide linkage at the same time (43).

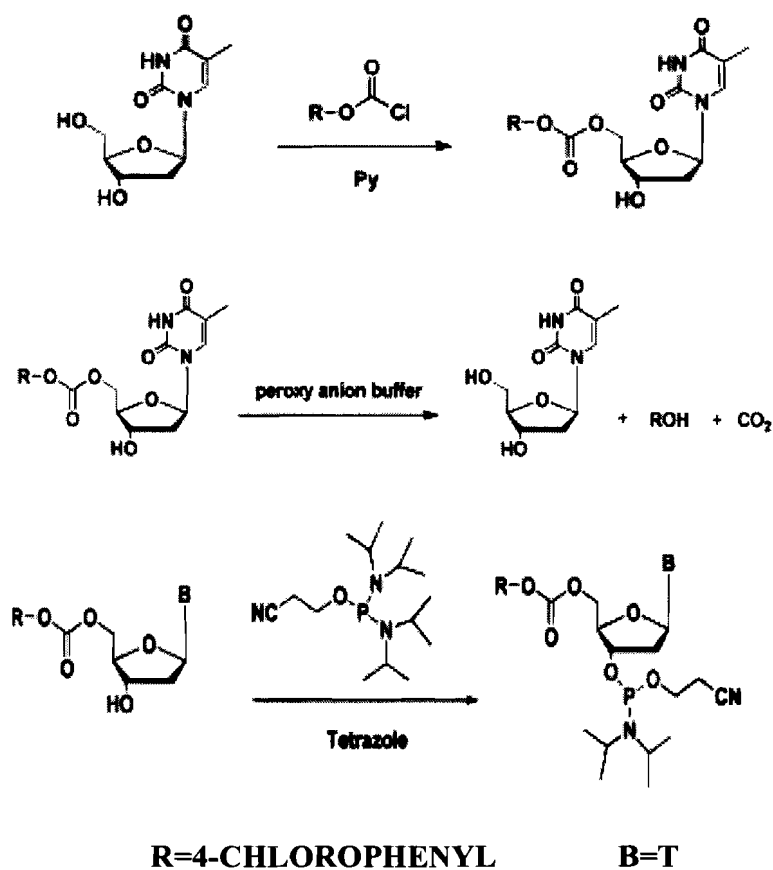


**Figure 18a.** Synthesis of phosphoramidite nucleotide

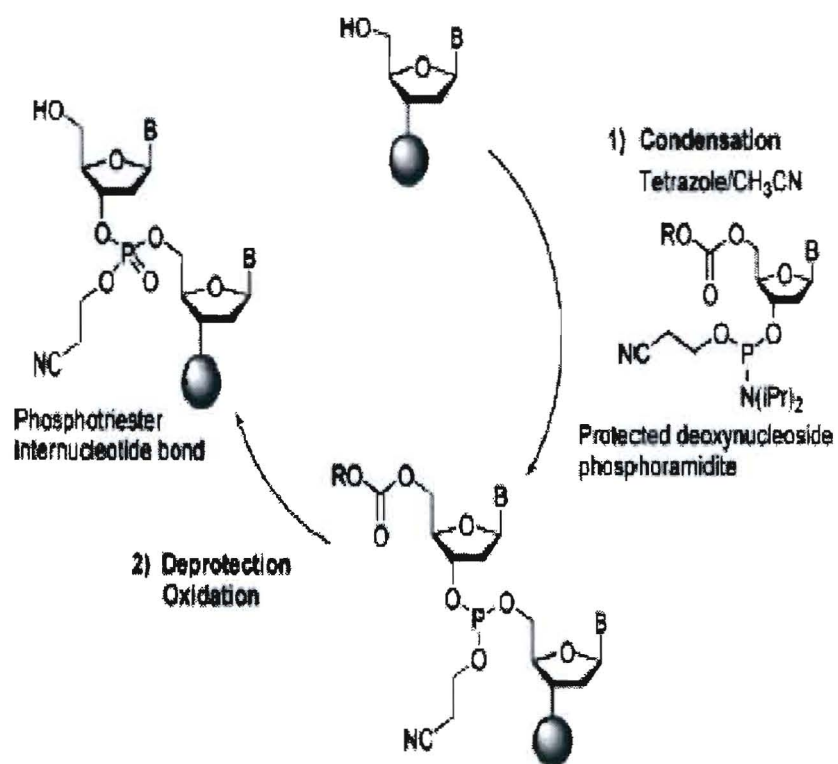


Figure 18b. New two step synthesis of ODN

## 11 SUMMARY OF THESIS

Small molecule complexes such as DOTA and DPTA that are used as MRI contrast agents cannot effectively distinguish diseased tissues from normal ones due to their fast removal from the body and the lack of specific body receptors for these molecules. It is therefore necessary to couple these molecules with those that can bind to receptors in the targeted body cells. However, these should be easy to synthesize and have very little toxicity in the body.

Folic acid is a natural agent that has been used in drug delivery and many other processes. Thus, our use of folic acid to target receptors is justified. Folate receptors are much more highly enriched in tumor or cancer cells than in normal cells. The aim of this thesis is to synthesize folate-linked oligonucleotide Gd-DOTA conjugates that will have a high tumor uptake and thus high MRI enhancement of targeted tumor cells.

## 12 EXPERIMENTAL

### MATERIALS

TLC was done on a pre-coated silica plate. Column chromatography was done with a glass column packed with, glass wool, sand, and 70-230 mesh 60A silica gel (Aldrich Chemical company, Milwaukee, Wisconsin). DOTA salt was purchased from Macrocycles, Inc. (Dallas, Texas). Evaporation was done using a rotary evaporator connected to a vacuum pump and a vacuum dessicator was used for the drying. NMR was run on a Perkin Elmer 60MHz instrument and UV measurement was done on a Cary 50 Bio UV-Visible spectrophotometer. DNA was synthesized with an Applied Biosystems 394 DNA/RNA Synthesizer at the University of Kansas Medical Center, Kansas City, Kansas.

### SYNTHESIS OF 5-METHOXYCARBONYLVINYL-2'-DEOXYURIDINE

5-iodo-2'-deoxyuridine (5.0g) was dissolved in 20ml of dioxane solvent. Triphenylphosphine (0.36g), palladium (II) acetate (0.15g), triethylamine (2.5ml) and methyl acrylate (2.43ml) were added. Argon gas was bubbled through the mixture to keep out moisture. The mixture was stirred for 24 hours at 70°C and then dissolved in a minimum amount of dioxane and left to crystallize overnight. TLC was done with 8.5:1.5 ethylacetate/ethanol and then purified by column chromatography using the same solvent. The solvent was then evaporated to obtain a yield of 2.5g (53%).

<sup>1</sup>HNMR in d-6 dimethyl sulfoxide at 60MHz:

2.0-2.75ppm (medium, multiplets), 3.0ppm (sharp, strong), 4.0-4.5ppm (small), 5.0-5.5ppm (small) 6.0-6.5ppm (small, multiplets), 7.0 – 7.5 ppm (small, sharp, multiplets), 7.5 –8ppm (medium multiplets), 8.55ppm (medium sharp), 11.75ppm (medium, sharp).

## **SYNTHESIS OF 5-METHOXYCARBONYLVINYL-5'-O-(DIMETHOXY TRITYL) -2'-DEOXYURIDINE**

5-Methoxycarbonylvinyl-2'-deoxyuridine (826mg) of was added to 12.5ml of pyridine along with 804mg of dimethoxytrityl chloride and argon gas was bubbled through the mixture for 5 minutes. The mixture was stirred at room temperature for twenty four hours to obtain a yellow precipitate. Ice cubes were added to this precipitate, followed by four extractions with 30ml of an ice cold, saturated solution of sodium bicarbonate ( $\text{NaHCO}_3$ ) and three more times with saturated sodium chloride solution. The bottom organic layer containing the sample was dried with powdered  $\text{CaCl}_2$  for 30 minutes.

The sample was then filtered through a glass wool and evaporated with the rotary evaporator. TLC of the sample was carried out with 9.5:0.5 methylene/methanol solvent and purified with column chromatography using the same solvent system. The solvent was evaporated from the eluate and the solid was dried under vacuum. The sample was dissolved in 3ml of methylene chloride, the solvent was evaporated again, and the product was dried under vacuum. The yield was 565mg (32%).

## **SYNTHESIS OF 5-[N(6-AMINOHEXYL)-3-(E)-ACRYLAMIDO]-5'-O-(DIMETHOXY TRITYL) -2'-DEOXYURIDINE**

5'-DMT-5-Methoxycarbonylvinyl-2'-deoxyuridine (565mg), hexamethylenediamine (3.006g), and 4-dimethylaminopyridine (0.01g), were dissolved in 10ml of methanol. The reaction was carried out under an argon atmosphere for three days at  $50^\circ\text{C}$ . The sample was then evaporated under vacuum. The sample was twice redissolved in 10ml methanol and the solvent was evaporated to obtain a yield of 250mg (38%).

**SYNTHESIS OF 5-[N(6-AMINOHEXYL)-3-(E)-ACRYLAMIDOTRIFLUORO ACETYL]-5'-O-(DIMETHOXY TRITYL)-2'-DEOXYURIDINE**

The previous sample, (5-[N (6-Aminohexyl)-3-(E)-acrylamido]- 5'-O-(dimethyltrityl)-2'-deoxyuridine, 136mg), was precipitated by mixing with anhydrous ethyl ether, then redissolved in methanol (20ml) and bubbled with argon gas. Liquid trifluoroacetic anhydride (0.5ml) was added to it and the mixture was stirred for two days at room temperature. The sample was mixed with 0.013g of 4-dimethyl amino-pyridine and 0.5ml of ethyltrifluoroacetate and stirred again for two days at room temperature. The white creamy precipitate was evaporated to dryness with the rotary evaporator. TLC was done with 8.5:0.5 methylene chloride/methanol and purified by column chromatography with the same solvent. The solvent was removed by rotary evaporation to obtain 197mg (65.2%) of product.

**SYNTHESIS OF 5-[N(6-AMINOHEXYL)-3-(E)-ACRYLAMIDO-TRIFLUORO ACETYL]-5'-O-(DIMETHOXY TRITYL-2-CYANOETHYLDIISOPROPYL CHLOROPHOSPHORAMIDITE)-2'-DEOXYURIDINE**

5-[N (6-Aminohexyl)-3-(E)-acrylamido]- trifluoroactete-5'-O-(dimethyltrityl)-2'-deoxyuridine (136mg) was dissolved in 10ml of tetrahydrofuran (THF) and 0.7ml of 2-cyanoethyl-diisopropyl-chlorophosphoramidite (chlorophosphoramidite), 1.5ml of N,N-diisopropylethylamine, 0.063g (63mg) of 4-dimethylaminopyridine were added. The mixture was stirred continuously under an argon atmosphere in an ice bath for one hour. The orange red mixture turned into a yellow solid. The mixture was stirred at room temperature for three hours. The sample was added to 30ml of ethyl acetate and extracted six times with 25ml of saturated NaHCO<sub>3</sub>

solution and then five times with 25ml of saturated NaCl solution. The final organic layer was separated out, dried with calcium chloride pellets, and the solvent was then removed with a rotary evaporator to obtain a yellowish solid. TLC was done in a solution of 5.0:1 ethylacetate/ethanol and then with 4:1 ethyl acetate/hexane. Column chromatography was done with the 4:1 ethyl acetate/hexane. TLC of the sample eluate was done with the same solvent system. Ethyl ether (1.0ml) was added to the sample and evaporated again. This was repeated for three times to obtain a yield of 90mg (49.5%) of product. <sup>1</sup>HNMR in CDCl<sub>3</sub> : 1.0-1.5ppm (strong sharp peaks; triplets), 2.0ppm (multiplets, small), 2.5-3.0 (quartet, medium), 3-3.5ppm (multiplets), 3.5-4.0ppm (sharp, medium).

#### **AUTOMATED DNA SYNTHESIS**

The Applied Biosystem 394 DNA/RNA Synthesizer was rinsed first with acetonitrile to flush out all impurities. Argon gas was pumped through the instrument to flush out all liquid and remaining impurities, including acetonitrile. Synthesis was carried out on 0.03g of solid Universal support in the Control Pore Glass (CPG) column support joined to 5'-DMT protected 2'-deoxythymidine. The DMT protecting group was removed with trichloroacetic acid followed by activation with tetrazole prior to coupling with the normal thymidine phosphoramidite. Oxidation of the phosphite to phosphate was done with a solution of aqueous iodine in pyridine. Deblocking, coupling, oxidation and capping were repeated until the oligo synthesis was complete. The product was rinsed with acetonitrile and treated with 1:1 the ammonia /methylamine to remove oligonucleotide from the CPG in the column.

The oligonucleotide consisted of ten nucleotides with the first, fourth, and eighth bases having the 6-hexylenediamine acrylamido groups at the 5-positions

while the rest are all 2'-deoxythymidine nucleotides, that is d[TTXTTTXTTTX], where X is the aminohexyl derivatized bases. This oligomer was synthesized on a 1.0 μmole scale, which coupled very successfully during the synthesis. However, it was denatured after purification and coupling of DOTA via condensation amidation with acrylamido hexylamine group on the oligo. A new DNA was synthesized using amino modifier 6-(4-Monothoxytritylamino) hexyl-(2-cyanoethyl)-(N,N-diisopropyl)-phosphate (or simply MMT C6 aminomodifier). The 5' position was occupied by a deoxythymidine nucleotide attached to the column support followed by coupling to 8 more thymidine nucleotides as done in the previous steps to make the nine unit oligomer. The decoupling or deprotection step after synthesis was done by adding a 100 μL of TEA (Triethylamine) and leaving the solution to stand for an hour followed by 17 hours at 40°C. Purification was done using two Poly Pak columns (52) by eluting with 3:7 CH<sub>3</sub>CN/CH<sub>2</sub>Cl<sub>2</sub> instead of the usual TFA to remove the detritylate. This was followed by addition of 80% CH<sub>3</sub>COOH to each column. The eluate was kept for an hour one at room temperature and then dried in a heating block and under an air stream. DNA was collected as white residue in 16 vials and kept frozen at -10 to -30°C.

## **DNA CONJUGATION AND PURIFICATION**

### **PREPARATION OF BICARBONATE BUFFER (pH 9)**

Anhydrous sodium carbonate (0.496g) was added to 8.4g of sodium bicarbonate (NaHCO<sub>3</sub>) and diluted to 100ml with distilled water.

### **PURIFICATION OF DNA**

The oligomer was dissolved in 0.15ml of acetonitrile and transferred into 1.5ml microcentrifuge plastic cartridges containing sephadex G-25 (SR Gel filtra-

tion cartridges (Edge Bioystems, Gathersburg, Maryland). The sample was centrifuged for three minutes in a Micro-centrifuge Model 235B. The filters were removed and the solvent was evaporated by using a Centrивap Concentrator (Lab Conco Corporation, Kansas City, Missouri) for six hours at 35°C.

### **PREPARATION OF DNA DOTA LINKER**

DOTA-NHS ester, PF<sub>6</sub> salt (30mg) was dissolved in 1.8ml of the Na<sub>2</sub>CO<sub>3</sub>/NaHCO<sub>3</sub> buffer. An aliquot (0.15ml) of this solution was added to each DNA sample and swirled around to mix well for one minute and allowed to stand for 3 hours. This was followed by 3 minutes of gel centrifuge filtration.

### **PREPARATION OF Gd (III) AQUEOUS SOLUTION**

GdCl<sub>3</sub> salt (3.717g) was dissolved in 10ml of distilled water.

### **EDTA SOLUTION**

Disodium EDTA salt (3.724 g) was dissolved in 20ml of distilled water to make a saturated solution.

### **PREPARATION OF Gd-DOTA DNA CONJUGATE**

The GdCl<sub>3</sub> solution, in 0.1ml aliquots, was added to each of the DNA solution to form a white creamy precipitate. Approximately 3 of drops of EDTA were added to each vial to dissolve the precipitate and form a clear solution. The sample was purified by sephadex G-25 gel filtration centrifugation for three minutes and then the solvent was evaporated in a centrifuge evaporator at 35°C for 14.5 hours. A pale, almost colorless, residue was obtained.

### **UV MEASUREMENTS**

The DNA was dissolved in 1.0ml of deionized water and 50µl of the resulting

solution was diluted to 1.0ml with distilled water. De-ionized water was used as the blank. This was repeated for the Gd-DOTA–oligomer conjugate and the intact Gd-DOTA complex, except that deionized water was replaced with a solution of buffer with 3 drops of EDTA solution. UV measurements were taken at 260nm in a Cary 50 Bio UV-Visible spectrophotometer using a 1.0 cm quartz cuvette. The results showed no prominent peak at 260nm. A new DNA was synthesized and its UV spectrum was measured which gave a prominent peak at 260nm.

## **GEL ELECTROPHORESIS**

### **PREPARATION OF SOLUTIONS**

#### **30% ACRYLAMIDE**

Acrylamide (38.003g) and bisacrylamide (2.044g) were dissolved to 100ml with distilled water.

#### **BUFFER**

Tris(hydroxyethyl)amine (THAM) (27.016g) and 18.515g Boric acid was dissolved to 500ml with distilled water.

#### **10% AMMONIUM PERSULFATE (APS)**

Ammonium persulfate (1.207g) was dissolved and diluted to 10ml with distilled water.

#### **ACRYLAMIDE–UREA POLYMER**

APS (450µl), 35µl of N, N', N'', N'''-tetramethylethylenediamine (TMEDA), 31.5g of urea, 37.5ml acrylamide and 15ml of TBE buffer were mixed for about 20 minutes to dissolve and quickly poured in between two tight glass plates. A comb was inserted at the top to create wells (or holes) and the gel was allowed to solidify.

## **DNA ELECTROPHORESIS**

An aqueous solution (20 $\mu$ l) of 185 $\mu$ g of DNA in 1.25ml was diluted with 20 $\mu$ l formamide buffer. The top of the plate was filled with TRIS buffer. The buffer (12ml) was injected into wells in the sandwiched polyacrylamide gel. A solution of Bromophenol blue dye in formamide was injected into another well besides that of the DNA to monitor the movement of DNA down the gel. Terminals of the electrophoresis cell (Bio-Rad Protean HX1 Cell) were connected and switched at 502V to begin the Electrophoresis, which took about 5 minutes to complete. The cell was stopped and the gel was removed from the glass plate and placed on a white fluorescent plate. Exposure of the plate to UV light showed no trace of DNA. This was repeated again but result was still negative. Another electrophoresis was done at a lower voltage (400V) with glycerol instead of formamide, but results was still negative. A new DNA strand was synthesized and the electrophoresis was measured again at 250V. This also gave a negative result due to insufficient amount of DNA on the column.

## **SYNTHESIS OF 6-FORMYLPTERIN**

Liquid HBr (6.0ml) (48 %) solution and 4.8ml of liquid bromine solution was added to 10.0g of folic acid. The mixture was stirred for two and a half hours at 93°C on an oil bath. The yellow solid was filtered and washed with distilled water and then with hot acetone. The solvent was evaporated from the filtrate with the rotary evaporator to obtain a yellow solid product (3.64g, 82.7%) while the filtrate residue gave a yield of 2.55g (58.6%). Both products were dried under vacuum.

Various chemical tests for the presence of the carbonyl group were inconclusive. Tollen's test showed a dark precipitate for the residue and an orange precipitate for the

filtrate. Propanal was used as reference. After boiling, the residue was much darker than the filtrate. Benedict's test showed a deep green color for the residue and dull green color for filtrate. After boiling, the filtrate became light brown while the residue became dark brown.

<sup>1</sup>HNMR in DMSO at 60MHz. [(filtrate: 5-5.5ppm (sharp, large), 8-9ppm (small), 2.5-3ppm (trace), residue: 8ppm (medium, sharp), 7-7.5ppm (medium, broad), 2.5ppm (small)].

### **SYNTHESIS OF N-ISOBUTYRYL-6-FORMYLPTERIN**

The filtrate (3.164g) was mixed with 158.2ml of isobutyric anhydride while 0.481g of the residue was also added to 20.55ml of the isobutyric anhydride. Each reaction mixture was bubbled with argon gas and stirred at 130°C for 30 hours. After this, the reaction mixture was allowed to cool down to room temperature (25°C). A dark brown precipitate was obtained for the residue while the filtrate was dark brown as before. The two samples were stored at 0°C in a refrigerator for twenty four hours.

Each sample was filtered and washed thoroughly with hexane and then with 1:1hexane/2-propanol. Unfortunately, there was no precipitate after filtration of both samples. However, the precipitate was later centrifuged and solvent was decanted off to obtain 1.90g (48.2%) of yellowish solid product, which was dried under vacuum. However, the residue did not produce any product.

### **SYNTHESIS OF FOLIC ACID SUCCINAMIDE ESTER**

Dimethylsulfoxide (DMSO) (40ml), dicyclohexylcarbodiimide (0.25ml) and 0.257g N-hydroxysuccinamide (NHS) were added to 2.0g of Folic acid.

The reaction flask was covered with aluminium foil to exclude light, due to the photosensitivity of the reaction. Argon gas was bubbled throughout the mixture for about a minute, the flask was capped, and the mixture was then stirred for 24 hours. A yellow precipitate was obtained; however, no precipitate residue was obtained after filtration. A solution of 7: 3 ethyl ether/acetone was added to the filtrate solution to form a creamy yellow precipitate and stirred for one hour at room temperature. The precipitate was filtered and washed with 10ml of acetone, followed by 10ml of diethylether and dried under vacuum. The yield was 2.30g (94%).

#### **SYNTHESIS OF 15, 16 –O- (ISOPROPYLIDENE)-4,7,10,13-TETRAOXAHEXADECYLAMINE FOLATE ESTER**

Liquid 15, 16 –O- (isopropylidene)-4, 7, 10, 13-tetraoxahexadecylamine (1.0g) was added to 1.676g of the freshly prepared sample and 70ml of previously dried pyridine was added to it. Argon gas was bubbled through the mixture for twenty minutes and the mixture was stirred for twenty four hours, after which the solvent was evaporated with a rotary evaporator. TLC was done with 1:9 methanol/methylene chloride. The sample was purified by column chromatography using the same solvent. TLC of the eluate showed it contained only one compound. The yellow eluate was filtered through glass wool and the solvent was evaporated with the rotary evaporator. The yield was 700mg (22%).

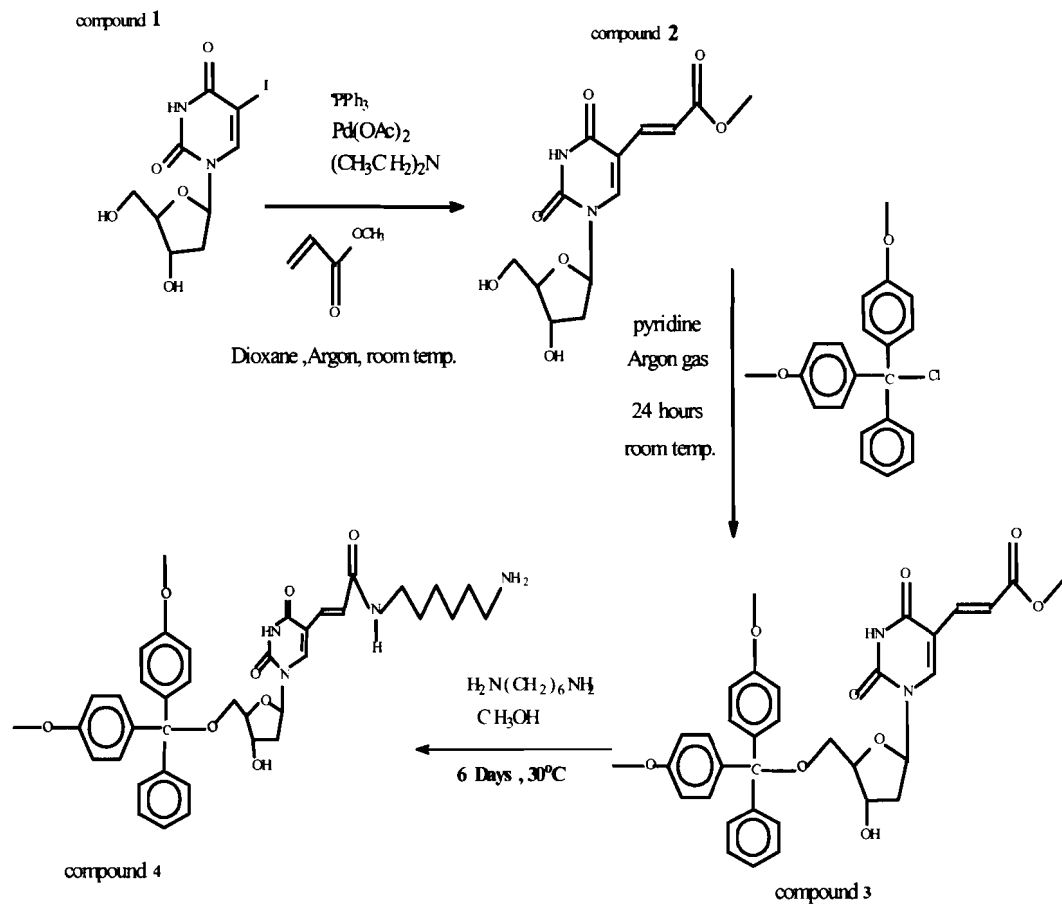
<sup>1</sup>HNMR in CDCl<sub>3</sub> (3 drops) and TMS at 60MHz:

0.5-0.75 ppm (small, multiplets), 2.50ppm (sharp, strong), 3.5-3.75ppm, (sharp, medium).

## 13 RESULTS AND DISCUSSION

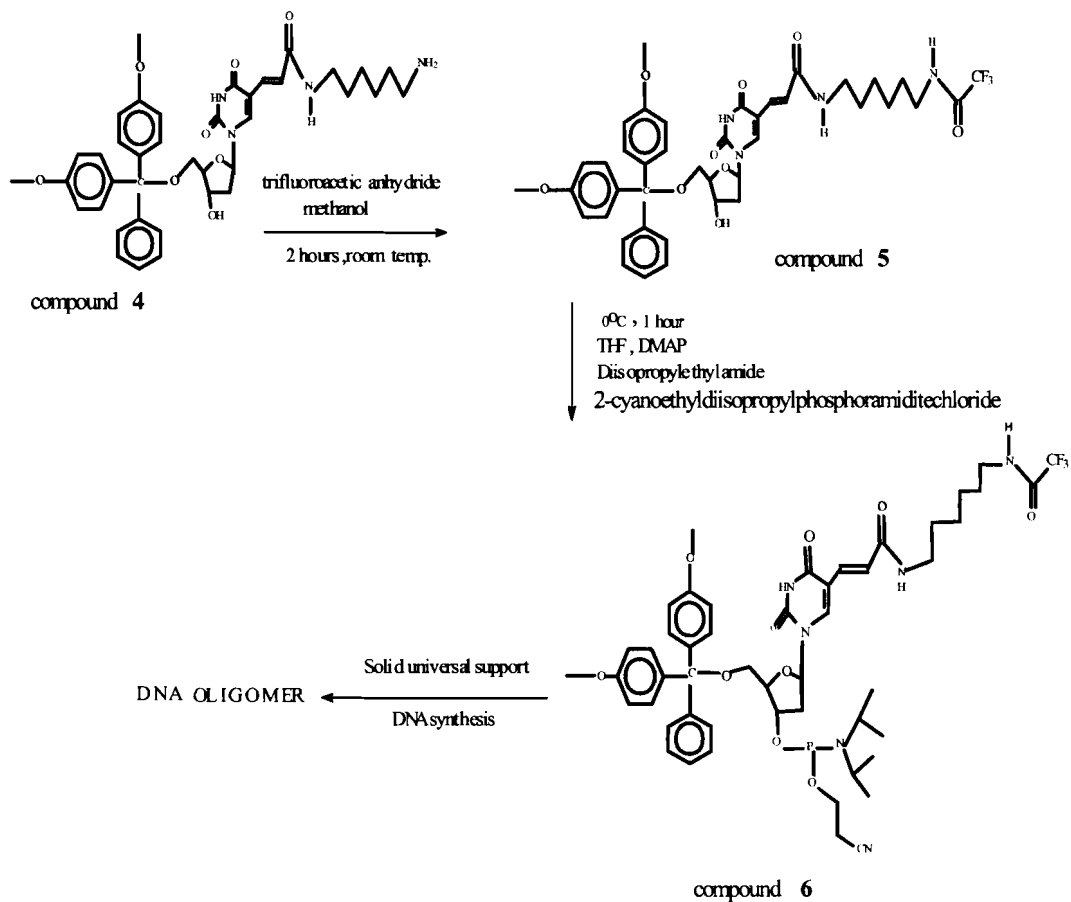
Compound **2** was prepared from 5-iodo-2'-deoxyuridine (compound **1**) using a Heck reaction. The reaction was carried out with triphenylphosphine ( $\text{PPh}_3$ ) and basic triethylamine  $(\text{CH}_3\text{CH}_2)_3\text{N}$  in dioxane solvent. The palladium acetate stabilizes the negatively charged iodide leaving group. Argon gas was used to exclude air and water in the reaction vessel. The 5' - position was coupled with Dimethoxytrityl (DMT) which serves as a good protecting group. This occurs in the presence of pyridine, since DMT is very stable in base. This under argon atmosphere to exclude any trace of acid vapor because DMT is acid labile. This led to formation of compound **3**. 1, 6-diamino-hexane was coupled to compound **3** via amide formation accompanied by elimination of a methoxy group at  $30^\circ\text{C}$  to form compound **4** (SCHEME I).

## SCHEME I



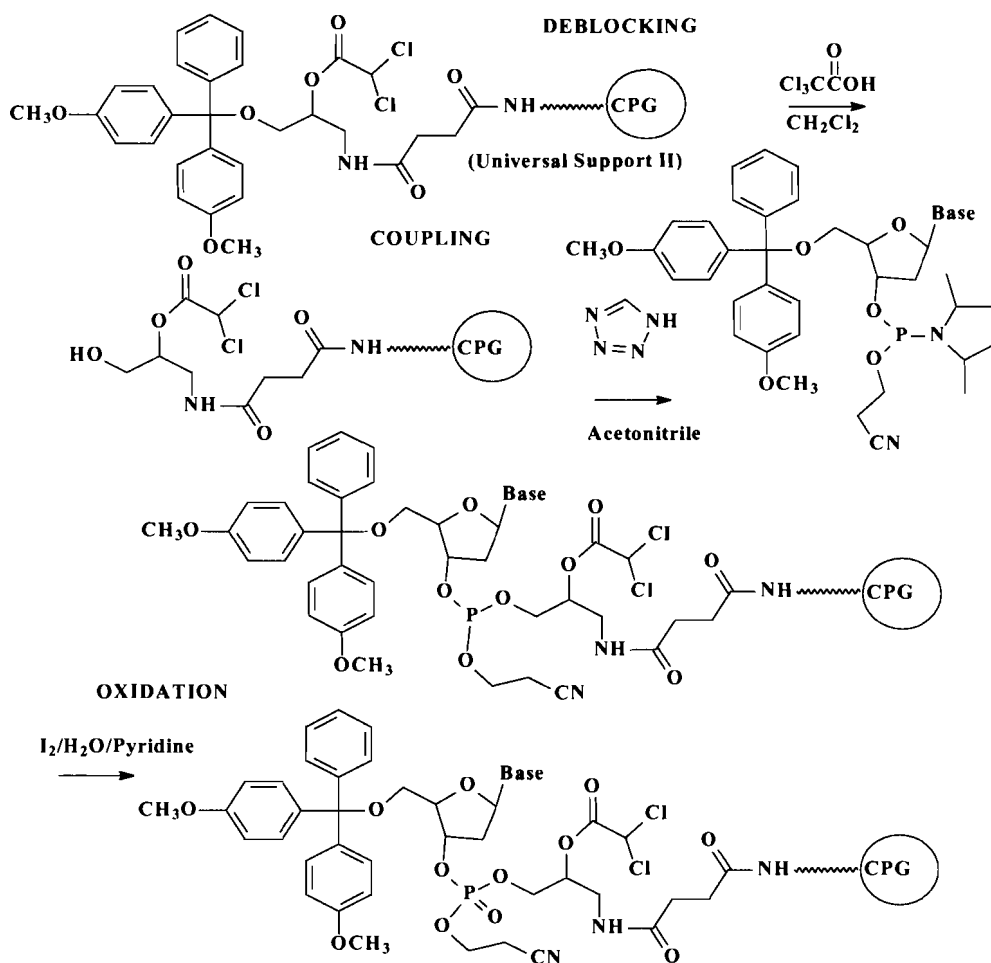
Compound 4 was reacted with trifluoroacetic anhydride in methanol to form trifluoroacetate derivative 6. The hydroxy group at 3'-position was converted into a phosphoramidite group by reaction with diisopropylethylamide and 2-cyanoethyl-diisopropylchlorophosphoramidite in THF and DMAP. This resulted in the formation of compound 6 (SCHEME II).

## SCHEME II



DNA synthesis (SCHEME III) yielded compound 7 (SCHEME IV). Deblocking was done by removal of DMT at 5'-position with trichloroacetic acid in methylene chloride. Coupling of the phosphoramidite of the nucleotide after activation of the hydroxyl (OH<sup>-</sup>) group of the linker with tetrazole. The weakly basic pyridine activates the removal of the proton. The diisopropylamine group was displaced and stabilized by pyridine.

## SCHEME III

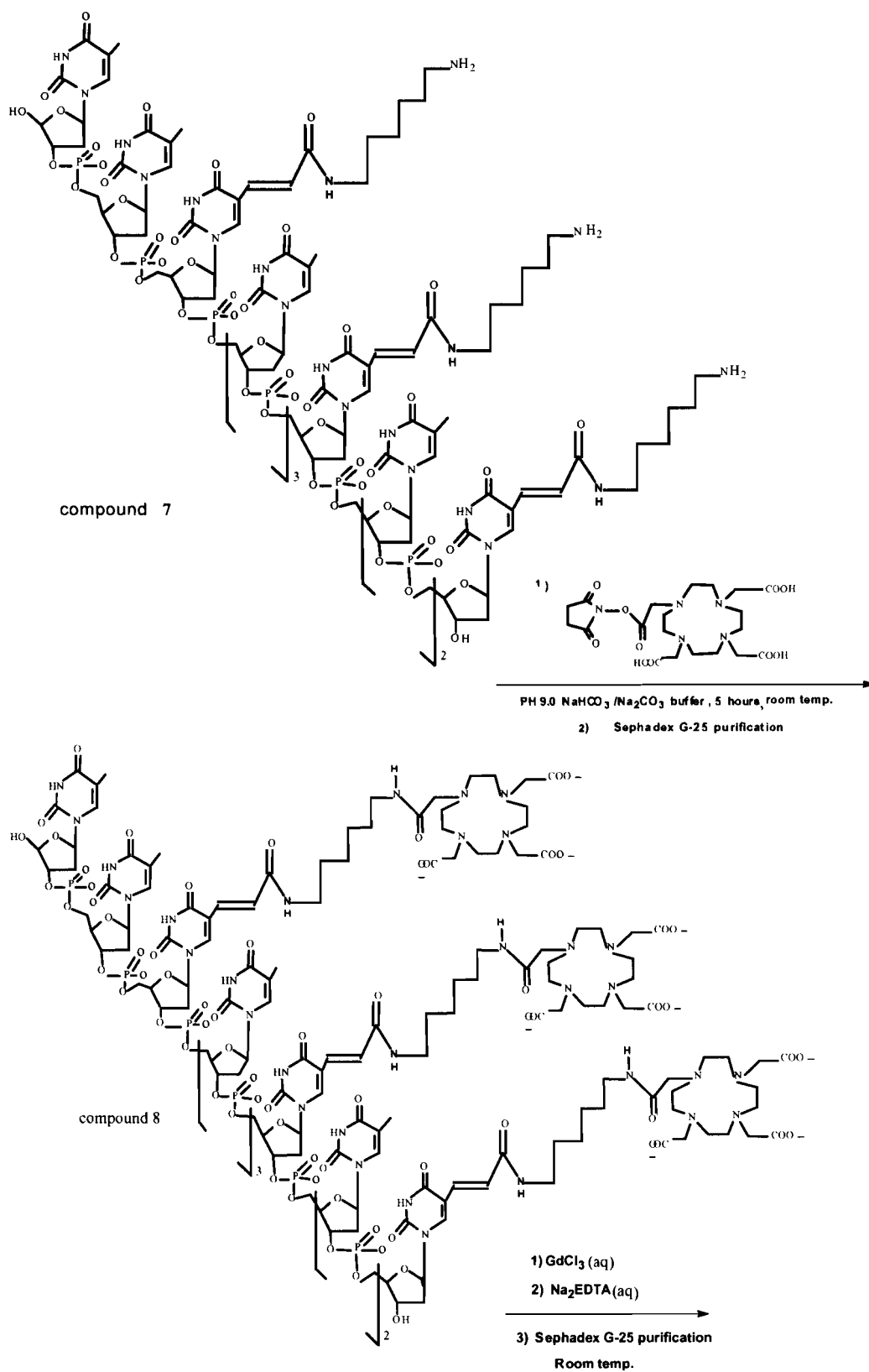


The oligomer was cleaved by treatment with a mild ammonium hydroxide.

Moreover, this also removed the TFA protecting group from the amino linker. This may have caused the oligomer to remain in the Poly-pak cartridge during purification.

A new oligo was synthesized using compound 4 as the starting nucleoside to yield compound 9 (Figure 19). This was purified by filtering through sephadex-G25 gel in a centrifuge for 3 minutes. The resulting solution was reacted with DOTA -NHS to couple the DOTA to the linker.

## SCHEME IV



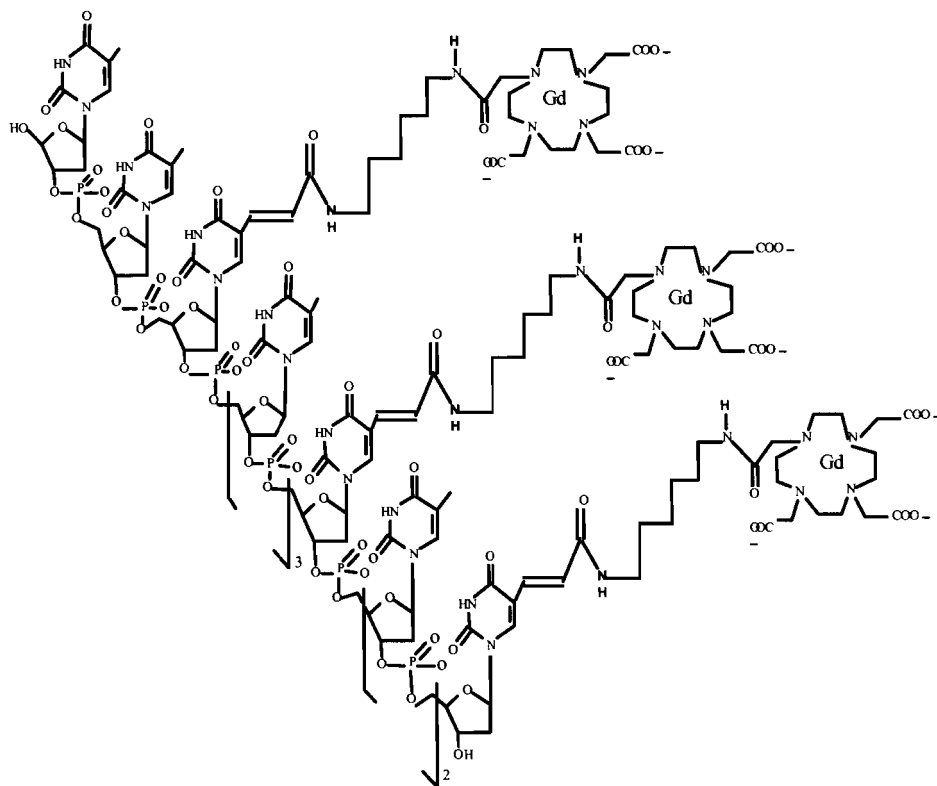


**Figure 19.** Structure of compound 9

Complexation with  $Gd^{3+}$  was done by reacting compound 9 with aqueous  $GdCl_3 \cdot H_2O$  solution  $Na_2CO_3/NaHCO_3$  buffer at pH 9. The thick cloudy precipitate dissolved after adding 2 drops of EDTA solution, which complexes the excess free  $Gd^{3+}$  ions. The resulting solution was filtered through sephadex G-25 again to obtain a pure oligonucleotide. The UV spectrum (see Figure 20) and the electrophoresis results revealed that the oligomer was denatured in storage.

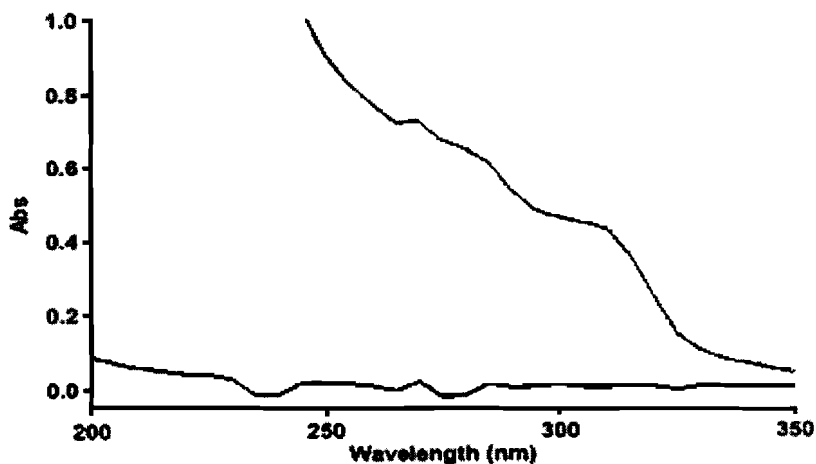


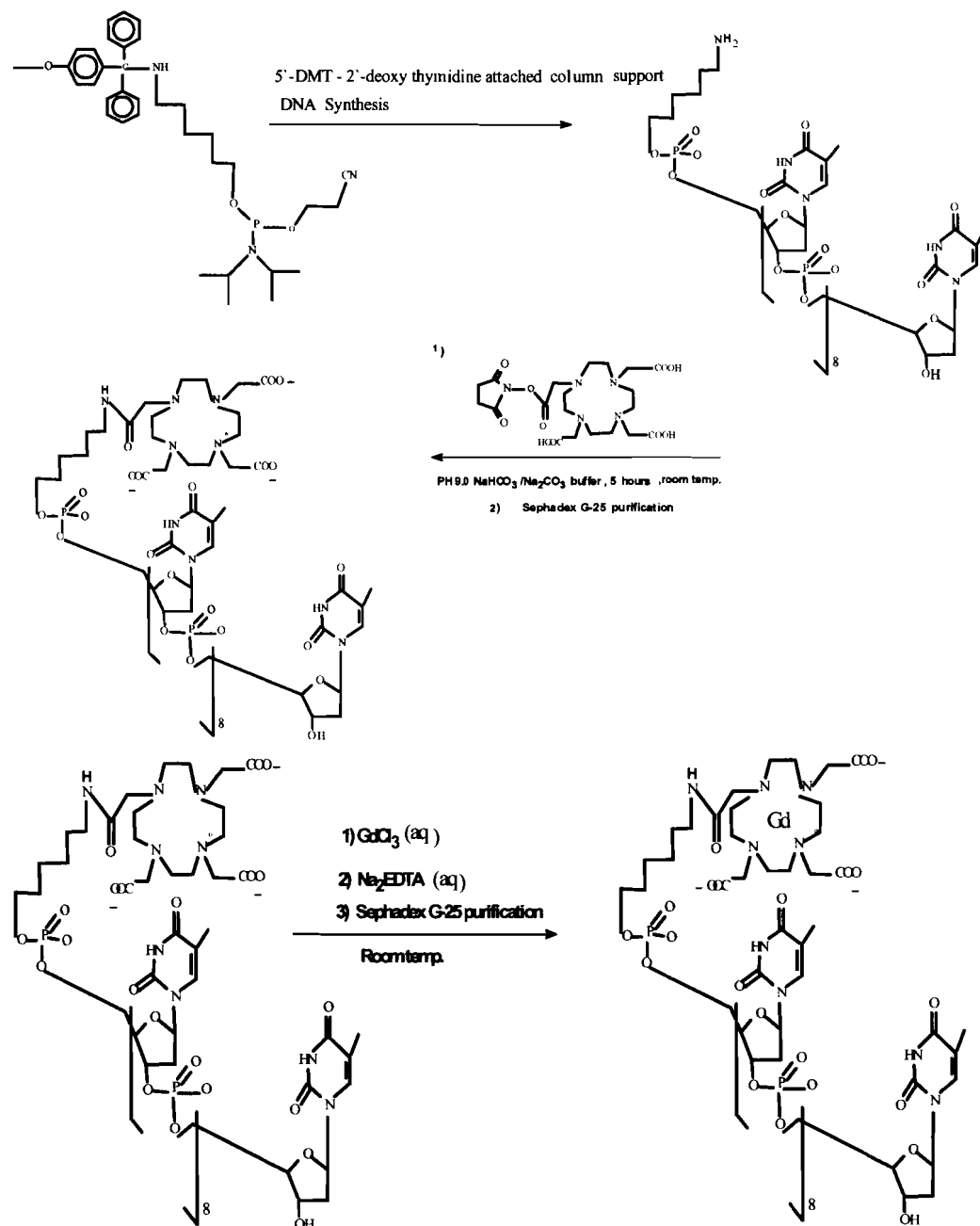
**Figure 20.** U.V. Spectrum of denatured DNA oligomer (bottom line is the blank absorbance of the buffer)

This could be due to unsuccessful Poly-pak purification in which the ammonium hydroxide that was used to cleave DNA from the column support removed the trifluoroacetyl group which was probably retained on the column. Thus, we were just working with a residue instead of the expected DNA. Other reasons could be, exposure to excessive heat during the centrifuge filtration and evaporation or the action of bacteria.

The second DNA sample was kept frozen and sterile after purification. The second DNA sample was already purified by poly pak, so it was not purified by gel filtration before reacting with the DOTA. The pH 9.0  $\text{CO}_3^{2-}/\text{HCO}_3^-$  buffer solution ensured that the DOTA remained ionized to complex the  $\text{Gd}^{3+}$  ion. Complexation is more effective under basic conditions since it avoids protons competing with metal ions for the negatively charged ligand binding sites. More time was allowed to enable the DOTA to couple effectively with the amino modifier on the DNA. The EDTA was added to remove excess unchelated  $\text{Gd}^{3+}$  ions. The Monomethoxy-trityl (MMT) functional group that was used required more acidic conditions to be

used for the deprotection than did DMT group the dimethoxytrityl.

### SCHEME V



The UV scan showed a very high absorbance of 0.177 at 260nm (Figure 21)

which is typical of an oligomer and this confirms that the DNA was not denatured.

However, the absorbance of the oligomer conjugated to Gd-DOTA

(Figure 22) complex seems to have been modified by absorbance of the Gd-DOTA complex (Figure 23). This resulted in a smaller peak at 260nm.

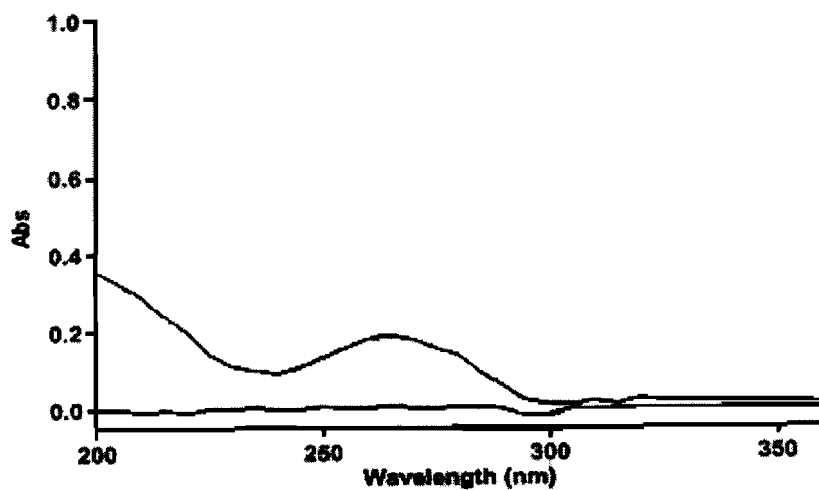


Figure 21. U.V. Spectrum of new oligo (active)

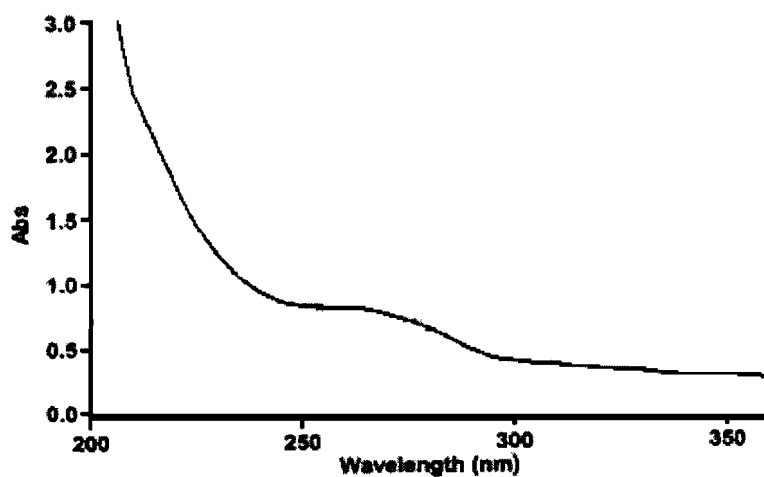
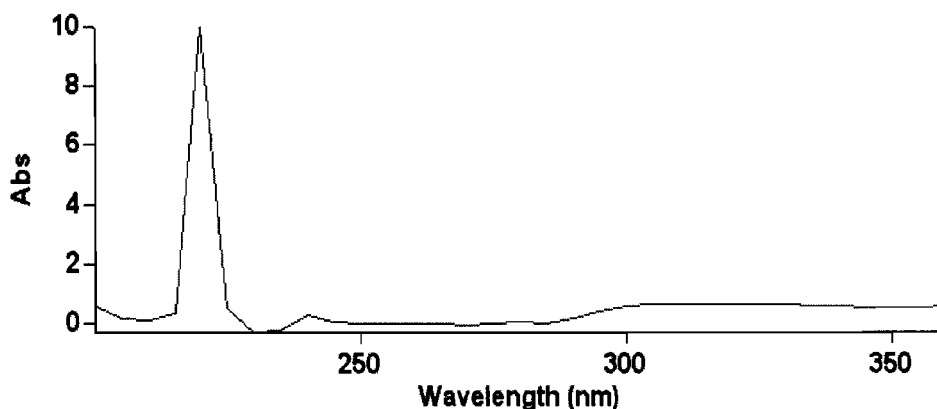


Figure 22. U.V. spectrum of oligomer coupled to Gd-DOTA complex

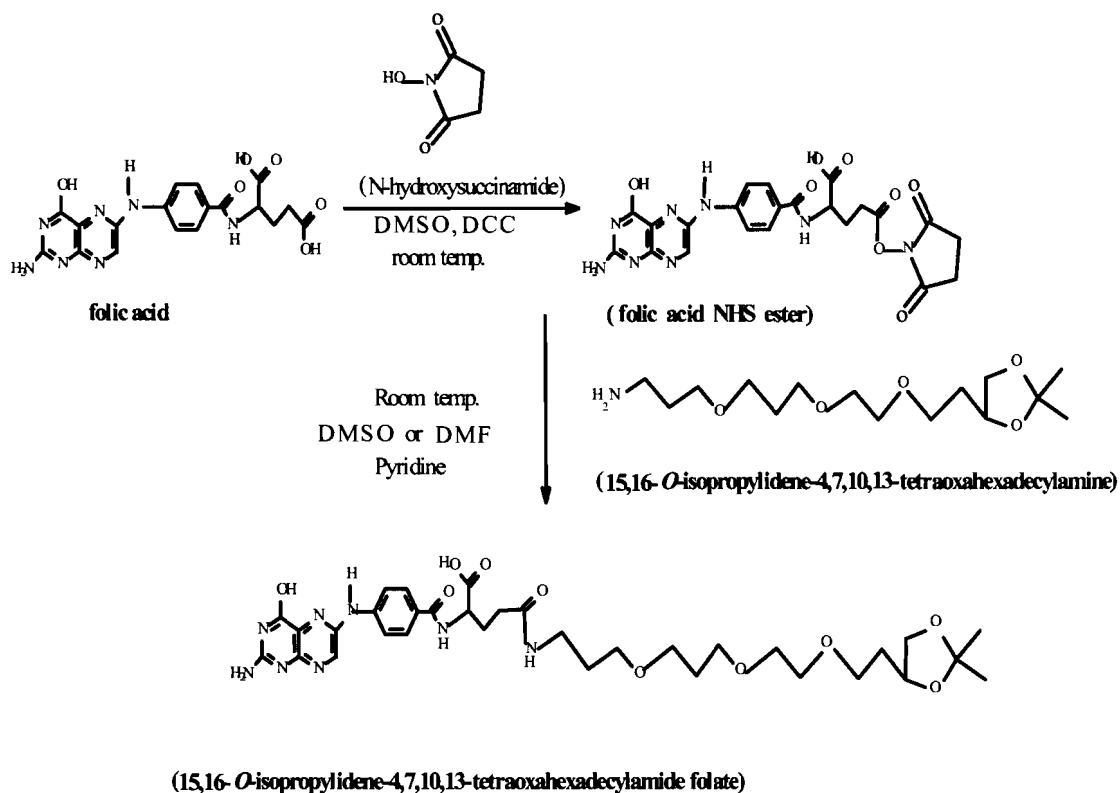


**Figure 23. UV Spectrum of Gd-DOTA Complex**

The amount of DNA (1.2mg) used in the electrophoresis was insufficient to give any detectable separation of components. Thus, nothing was seen in the gel electrophoresis.

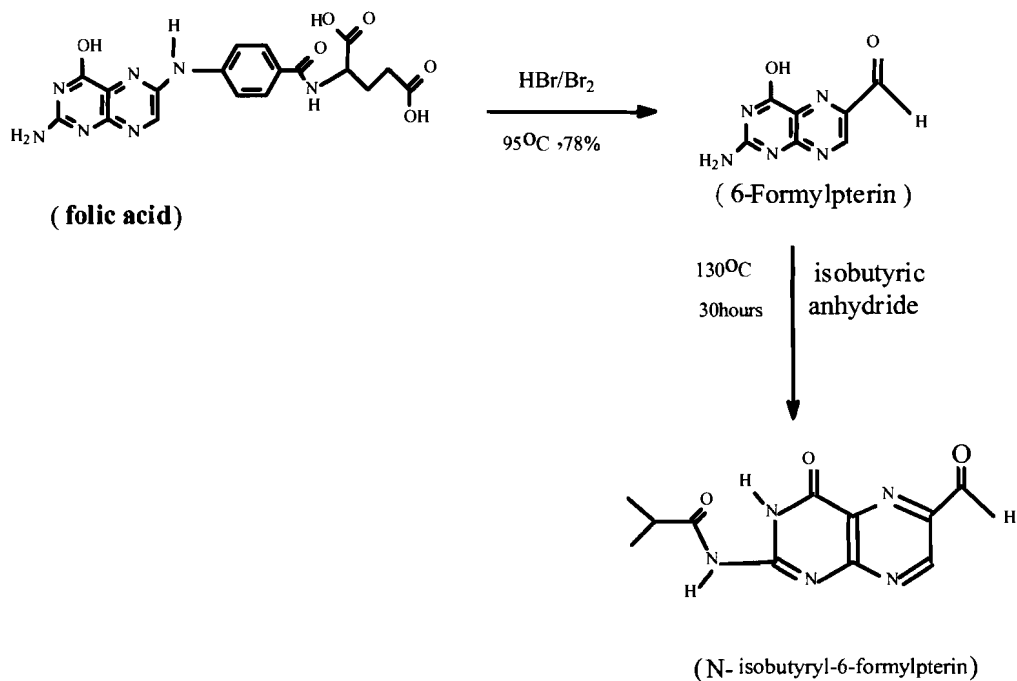
The reaction synthesis with folic acid (SCHEME VI and VII) was kept in darkness due to the photosensitivity of the folic acid. The  $\gamma$ -carboxyl group of the folic acid was protected by reacting with NHS in a basic solution of DCC. This is a condensation reaction with elimination of a water molecule in which NHS-couples exclusively at the less sterically hindered  $\gamma$ -carboxyl group. This yellow sticky precipitate was reacted with 15, 16-*O*-(isopropylidene)-tetradecylamine via an amide linkage with elimination of NHS group. This reaction was run in DMSO under an argon atmosphere. This was characterized by TLC and NMR.

## SCHEME VI



The compound was supposed to be coupled to the oligodecamer to facilitate cellular uptake by folate receptor enriched tumor cells. Other compounds were synthesized from folic acid included yellow 6-formylpterin and subsequent coupling with isobutyric anhydride at 130°C to form yellowish solid (N-Isobutyryl-6-formylpterin) (SCHEME VII). The latter compound was obtained by centrifugation, since filtration did not give any precipitate.

## SCHEME VII



The first oligodecamer that was synthesized had but purification was unsuccessful. Thus, the Gd(III)DOTA complex was not conjugated to the expected oligomer. The new oligomer had an amino linker that contained an 5'-MMT group (instead of TFA) which was removed after cartridge purification. The folic acid could not be coupled because we were not successful in obtaining an oligo with two amino linkers.

## 14 CONCLUSION

MRI has surely emerged as one of the greatest diagnostic techniques in medicine. The ability of this non-invasive technique to give three dimensional images of both hard and soft tissues without the danger of ionizing radiation or permanent physical injuries to patients makes MRI very safe to use. However, more needs to be done to improve the sensitivity and accuracy of MRI. Agents for drug delivery are also being utilized to deliver MRI agents to their targets.

The primary aim of this work was to synthesize  $Gd^{3+}$ -DOTA conjugated to an oligonucleotide that was coupled to a folate linker, (15,16-*O*-(isopropylidene)-tetradecylamidide folate. This was to promote selective uptake of the agent by tumor cells and enhance the corresponding MRI image. However, the folate linker was yet to be attached. It is expected that the high molecular weight would cause it to be retained in the vascular vessels thereby prolonging the imaging window of the compound. The slower rotational speed would enhance relaxation. The agent should be easily degraded and excreted from the body.

The oligodeoxynucleotides were sensitive to heat, while the folic acid derivatives were sensitive to light. Despite the precautions that were taken, these were difficult syntheses. Based on the theoretical considerations described earlier, the conjugate that was prepared should perform its intended functions very well.

**REFERENCE**

- 1) Lauffer, R.B. Paramagnetic metal complexes as water proton relaxation agents for NMR imaging: theory and design. *Chem. Rev.* **1987**, *7*, 901-927.
- 2) Caravan, P.; Ellison, J. J.; McMurry, T. J.; and Lauffer, R. B. Gadolinium(III) chelates as MRI contrast agents: Structure, dynamics, and applications. *Chem. Rev.* **1999**, *9*, 2293-2352.
- 3) Wang, X.; Jin, T.; Comblin, V.; Lopez-Mut, A.; Merciny, E.; Desreux, J.F. A kinetic investigation of the lanthanide DOTA chelates. Stability and rates of formation and of dissociation of a macrocyclic gadolinium (III) polyaza-polycarboxylic. MRI contrast agent. *Inorg. Chem.* **1992**, *31*, 1095-9.
- 4) Kumar, K.; Tweedle, M.F. Ligand basicity and rigidity control formation of Macrocyclic polyamino carboxylate complexes of gadolinium (III). *Inorg. Chem.* **1993**, *32*, 4193-9.
- 5) Brucher, E.; Sherry, A.D. Kinetics of formation and dissociation of the 1, 4, 7-triazacyclononane-N, N', N''-triacetate complexes of yttrium(III), gadolinium (III), and erbium(III) ions. *Inorg. Chem.* **1990**, *29*, 1555-9.
- 6) Kumar, K.; Chang, C.A.; Tweedle, M.F. Equilibrium and kinetic studies of lanthanide complexes of polyamino carboxylates. *Inorg. Chem.* **1993**, *32*, 587-93.
- 7) Kumar, K.; Jin, T.; Wang, X.; Desreux, J.F.; Tweedle, M.F. Effect of Ligand Basicity on the Formation and Dissociation Equilibria and Kinetics of Gd<sup>3+</sup> Complexes of Macrocyclic Polyamino carboxylates. *Inorg. Chem.* **1994**, *33*, 3823-9.
- 8) Aime, S.; Botta, M.; Ermondi, G.; Terreno, E.; Anelli, P.L.; Fedeli, U.; Uggeri, F. Relaxometric, Structural, and Dynamic NMR Studies of DOTA-like Ln(III) Complexes (Ln = La, Gd, Ho, Yb) Containing a *p*-Nitrophenyl Substituent. *Inorg. Chem.* **1996**, *35*, 2726-36.
- 9) Rebizak, R.; Schaefer, M.; Dellacherie, E. *Bioconjugate. Chem.* **1997**, *8*, 605-610.
- 10) Corot, Schaefer, M.; Beaute, S.; Bourrinet, P.; Zehaf, S.; Benize, V.; Sabatou, M.; Meyer, D. *Acta. Radiologica* **1998**, *9*, 94-99.
- 11) Rebizak, R.; Schaefer, M.; Dellacherie, E. *Bioconjugate. Chem.* **1997**, *8*, 605-610.
- 12) Sieving, P.F.; Watson, A.D.; Rocklage, S.M. Preparation and characterization of paramagnetic polychelates and their protein conjugates. *Bioconjugate. Chem.* **1990**, *1*, 65-71.

- 13) Shuang, Liu and Scott Edwards. Bifunctional Chelators for Therapeutic Lanthanides Radiopharmaceuticals. *Bioconjugate Chem.* **2001**, *12*, 7-34.
- 14) Kenneth N. Raymond and Valerie C. Pierre. Generation, High Relaxivity Gadolinium MRI Agents. *Bioconjugate Chem.* **2005**, *16*, 3-8.
- 15) Kumar Krishan; Allen Chang; Francesconi L.C.; Dischino D.D.; Marley M.F.; Gougoutas J.Z.; Tweedle M.F. Synthesis, Stability, and Structure of Gadolinium (III) and Yttrium (III) Macrocyclic Poly(amino carboxylates). *Inorg. Chem.* **1994**, *33*, 3567-3575.
- 16) Cacheria, W.P.; Sherry, A.D. Thermodynamic study of lanthanides complexes of 1,4,7-triazacyclo-nonane-N,N'N''-triacetic acid and 1,4,7,10-tetraazacyclododecane-N, N', N'', N'''-tetraacetic acid. *Inorg. Chem.* **1987**, *26*, 958.
- 17) Loncia, M. F.; Deareux, J.F.; Mercini, E. Coordination of lanthanides by two polyamino polycarboxylic macrocycles: formation of highly stable lanthanide Complexes. *Inorg. Chem.* **1986**, *25*, 2646.
- 18) Yu-Hua Qi; Qing-You Zhang and Lu Xu. Correlation Analysis of the structure and Constants of Gadolinium (III) Complexes. *J. Chem. Inf. Comput. Sci.* **2002**, *42*, 1471-1475.
- 19) Scheinberg, D.A.; Strand, M.; and Gansow, O.A. Tumor imaging with radioactive metal chelates conjugated to monoclonal antibodies. *Science* **1982**, *215*, 1511.
- 20) Brasch, R.C.; Weinman, H-J.; Wesbey, G.E. *AJR, Am.J.Roentgenol.* **1984**, *142*, 625.
- 21) McNamara, M.T.; Tscholakoff, D.; Revel, D.; et al. (Radiology, Easton, Pa) **1986**, *58*, 65.
- 22) Anelli Pier Lucio; Latuana Luciano; Gabellini Milena; and Recanati Paola. DOTA Tris (phenylmethyl) Ester: A new Useful Synthone for the Synthesis of DOTA Monoamides Containing Acid-Labile Bonds. *Bioconjugate Chem.* **2002**, *12*, 1081-1084.
- 23) Li, M., and Meares, C.F. Synthesis, metal chelate stability studies, and enzyme digestion of a peptide-linked DOTA derivative and corresponding radiolabeled immunoconjugates. *Bioconjugate Chem.* **1993**, *4*, 275-283.

- 24) Lewis, M.R.; Raubitschek, A.; and Shively, J.E. A Facile, water –soluble method for modification of proteins with DOTA. Use of elevated temperature and optimized pH to achieve high specific chelate stability in radio-labeled immunoconjugates. *Bioconjugate. Chem.* **1994**, *5*, 565-576.
- 25) Rong Zheng Lu; Wang Xinghe; Parker Dennis L.; Goodrich K. Craig; and Buswell Henry R. Poly (L-Glutamic acid) Gd(III)-DOTA Conjugate with a Degradable Spacer for Magnetic Resonance Imaging. *Bioconjugate. Chem.* **2003**, *14*, 715-719.
- 26) Joseph Hornak, P. The Basics of MRI. **1994-2004**.
- 27) Witjes Han; Simonetti Arjan W.; Buydens Lutgarde. Better Brain Imaging with Chemometrics. *Anal. Chem.* **2001**, *1*, 548-556.
- 28) James Mattson and Merrill Simon. The Pioneers of NMR and Magnetic Resonance in Medicine: The Story of MRI. Jericho & New YORK: Bar-Ilan University Press, **1996**. ISBN 0961924314. (<http://www.ismrm.org>).
- 29) Rebizak, R.; Schaefer, M.; and Dellacherie, E. Polymeric conjugates of Gd<sup>3+</sup>- diethylenetriaminepentaacetic acid and dextran 2. Influence of spacer arm length and conjugate molecular mass on the properties and some biological parameters. *Bioconjugate Chem.* **1998**, *9*, 94-99.
- 30) Britz-Cuningham Scott H.; Adelstein James S. Molecular Targeting With Radionuclides: State of the Science. *Journal of Nuclear Medicine* **2003**, *44*, 1945-1961.
- 31) Olga Aronov; Aviva T. Horowitz; Alberto Gabizon; Dan Gibson. Folate-Targeted PEG as a Potential Carrier for Carboplatin, Analogs. Synthesis and in Vitro Studies. *Bioconjugate. Chem.* **2003**, *14*, 563-574.
- 32) Frey, U.; Ranford, J.D.; and Sadler, P.J. Ring-Opening reactions of the Anticancer Drug Carboplatin-NMR Characterization of Cis-[Pt-(NH<sub>3</sub>)-2(Cbdca- O) (5'-GmpN7)] in solution. *Inorg. Chem.* **1993**, *32*, 1333-1340.
- 33) Blommaert, F.A.; van Dijk-Knijnenburg, H.C.; Dijt, F.J.; den Engelse, L.; Baan, R.A.; Berends, F.; and Fichtinger-Schep, A.M.. Formation of DNA Adducts by the anticancer drug carboplatin: different nucleotides sequence preferences in vitro and in cells. *Biochemistry.* **1995**, *34*, 8474-8480.
- 34) Anderson, R.G.; Kamen, B.A.; Rothberg, K.G.; and S.W. Protocytosis: sequestration and transport of small molecules by caveolae. *Science* **1992**, *255*, 410-411.

- 35) Rothberg, K.G.; Ying, Y.S.; Kolhouse, J.F.; Kamen, B.A.; Anderson, R.G. The glycopospholipid –linked folate receptor internalizes folate without entering the clathrin-coated pit endocytic pathway. *J.Cell.Biol.* **1990**, *110*,637-649.
- 36) Mulder Willem J.M.; Strijkers Gustav J.; Griffioen Arjan W.; Bloois Louis van, Storm Grietje Molema, Gert, Koning Gerbern A.and Nicolay Klaas.A. Liposomal System for Contrast-Enhanced Magnetic Resonance Imaging of Molecular Targets. *Bioconjugate Chem.* **2004**, *15*,799-806.
- 37) Oyewumi Moses O. and Mumper Russell.J.Engineering Tumor–Targeted Gadolinium Hexanedione Nanoparticles for Potential Application in Neutron Capture.*Bioconjugate.Chem.***2002**, *13*, 1328-1335.
- 38) Lee, R.J.and P.S. Delivery of liposomes into cultured KB cells via folate receptor –mediated endocytosis. *J.Biol.Chem.* **1994**, *369*, 3198-3204.
- 39) Lee Robert J. and Low Philips S. Delivery of Liposomes into Cultured KB Cells Via Folate Receptor –Mediated Endocytosis. *J. Biol. Chem.***1994**, *269*, 3198-3204.
- 40) Kohler Nathan; Fryxell Glen E.; and Zhang Miqin. A Bifunctional Poly(ethylene glycol) Silane Immobilized on Metallic Oxide Nanoparticle for Conjugation with Cell Targeting Agents. *J.AM.CHEM.SOC.***2004**, *126*, 7206-7211.
- 41) Wang Susan, Lee Robert J.; Marthias Carla J.; Green Mark A. and Low Philip S. Synthesis, Purification, and Tumor Cell Uptake of Ga-Deferoxamine-Folate, a Potential Radiopharmaceutical or Tumor Imaging. *Bioconjugate Chem.***1996**, *7*, 56-62.
- 42) Vogel Karen; Susan Wang; Robert J.Lee; Jean Chmielewski; PhilipLow,S. Peptide–Mediated Release of Folate–Targeted Liposomes Content from Endosomal Compartments. *J.AM.CHEM.SOC.***1996**, *118*, 1581-1586.
- 43) Sierzchala Agnieszka B.; Deilinger Douglas J.; Betley Jason R.;Wyrzykiewicz Tadeusz, K.; Yamada Christina M. and Caruthers Marvin M. Solid-Phase Oligodeoxynucleotide Synthesis: A Two-Step Cycle Using Peroxy Anion Deprotection, *J.AM.CHEM.SOC.***2003**, *125*, 13427-13441.
- 44) Gabizon Alberto, Horowitz Aviva T.; Goren Dorit; Tzemach Dinah; Mandelbaum –Shavit Frederika, Qazen Masoud M.; Zalipsky Samuel. Targeting Folate Receptor with Folate Linked to Extremities of Poly-(ethylene glycol)-Grafted Liposomes: In Vitro Studies. *Bioconjugate Chem.* **1999** ,*10* ,289-298.

- 45) Kotchetkev,R.;Roschel,R.;Gmeiner ,W.; Kriivtchik,A.; Trump, E.; Bitsova, M.;Cinatl, J.; Kornhuber,B.; Cinatl,J. Antineoplastic Activity of a Novel Multimeric Gemcitabine-Monophosphate Prodrug Against Thyroid Cancer.*Anticancer. Research* **2000**, *20*, 2915-2922.
- 46) Zalipsky,S.; Puntambekar,B.;Bolikas,P.; Engbers,C.M.; and Woodle,M.C. Peptide attachment to extremities of liposomal surface grafted PEG chains Preparation of the long-circulating form of laminin pentapeptide, YIGSR. *Bioconjugate. Chem.***1995**, *6*,705-708.
- 47) Lee, R.J.; and Low, P.S. Delivery of liposomes into cultured KB cells folate receptor-mediated endocytosis. *J.Biol.Chem.* **1994**, *269*, 3198-3204.
- 48) Wong, S.; Lee R.J.; Mathias, C.J; Green, M.A. and tumor cell uptake of <sup>67</sup>Ga-desferoxamine-folate, a potential radiopharmaceutical for tumor imaging. *Bioconjugate. Chem.***1996**,*7*, 56-62.
- 49) Gmierner, W.H.; Trump, E.L; Wei C. Enhanced DNA-Directed Effects of FdUMP[10] Compared to 5FU.*Nucleotides ,Nucleoside,Nucleic Acids*, **2004**, *23*,401- 410,
- 50) Lasic,D.D.; and Needham,D. The “stealth” liposome: A prototypical biomaterial.*Chem.Rev.* **1995**,*95*,2601-2628.
- 51) Xing Q.Pan; Wang Huaqing; Shukla Supriya; Sekido Masaru; Dianne, M. Adams; Tjarks Werner; Barth Rolf F.; Lee Robert J. Boron-Containing Folate Receptor- Targeted Liposomes as Potential Delivery Agents for Neutron Capture Therapy. *Bioconjugate Chem.***2002**. *13*, 435-442.
- 52) User guide to DNA purification, Glen Research, Virginia.
- 53) Zalipsky Samuel ; Mullah Nasreen; Harding Jennifer A.; Gittelman Joshua.; Guo Luke; and Defrees Shawn A. Poly(ethylene glycol )-Grafted Liposomes with Oligopeptide or Oligosaccharide Ligands Appended to the Termini of the Polymer Chains. *Bioconjugate. Chem.* **1997**, *8*,111-118.
- 54) Barbeau, A. Manganese and extrapyramidal disorders. *Neurotoxicology* **1984**, *5*,1,13.
- 55) Sherry Dean.; Rodney D.; Brown III, Gerald Carlos .F.G.C.; Koenig Seymour, H. Kuan.; Kah-Tiong,;and Spiller Marga. Synthesis and Characterization of the Gadolinium(3+) Complex of DOTA -Propylamide :A Model DOTA -Protein Conjugate. *Inorg. Chem.***1989**, *28*,620-622.

- 56) Keire David, A. ; and Kobayashi Mitsuo. Nmr studies of the Metal– Loading Kinetics and Acid-Base Chemistry of DOTA and Butylamide –DOTA. *Bioconjugate. Chem.* **1999**, *10*, 454-463.
- 57) Loncin, M.F.; Desreux, J.F.; and Merciny, E. Coordination of lanthanides by two polyaminopolycarboxylic macrocycles: formation of highly stable lanthanide complexes. *Inorg. Chem.* **1986**, *25*, 2646-2648.
- 58) Cacheris, W.P.; Nickle, S.K.; Sherry, A.D. Thermodynamic study of lanthanide complexes of 1,4,7-triazacyclononane-N,N',N''-triacetic acid and 1,4,7,10-tetraazacyclododecane –N, N', N'', N''' -tetraacetic acid. *Inorg. Chem.* **1986**, *26*, 958-960.
- 59) Wang, X.; Jin, T.; Comblin, V.; Lopez-Mut, A.; Merciny, E.; and Desreux, J.F. A kinetic investigation of the lanthanide DOTA chelates. Stability and rates of formation of and dissociation of a macrocyclic gadolinium(III) polyazapolycarboxylic contrast agent. *Inorg. Chem.* **1992**, *31*, 1095-1099.
- 60) Desreux, J.F. Nuclear magnetic resonance spectroscopy of lanthanide complexes with tetraacetic tetraazamacrocycle . Unusual conformation properties. *Inorg. Chem.* **1980**, *19*, 1319-1324
- 61) Kodama, M.; Koike, T.; Mahatma, A.B.; and Kimura, E. Thermodynamic and kinetic studies of lanthanide complexes of 1,4,7,10,13-aazacyclopentacyclopentadecane-N,N',N'',N''', N''''-pentaacetic acid and 1,4,7,10,13,16-pentaacetic acid and 1,4,7,13,16-hexaazacyclooctadecane –N,N',N'',N''',N'''' , N''''''-hexaacetic acid. *Inorg. Chem.* **1991**, *30*, 1270-1273.
- 62) Stimuel, J.B.; Stockstill, M.E; and Kull, F.C.J. Yttrium-90 chelation properties of tetraazacetic acid macrocycles , diethylenetriaminepentaacetic acid analogues and novel terpyridine acyclic chelator. *Bioconjugate Chem.* **1995**, *6*, 219-225.
- 63) Lewis, M.R.; Raubitschek, A.; and Shively, J.E. A facile, water soluble method for modification of proteins with DOTA. Use of elevated temperature and optimized pH to achieve high stability in radiolabeled immunoconjugates. *Bioconjugates. Chem.* **1994**, *5*, 565-576.
- 64) Govindan, S.V.; Shih, L.B.; Goldenberg, D.M.; Sharkey, R.M. Karacay, H. Donnelly, J.E.; Losman, M.J.; Hansen, H.J.; and Griffiths, G.L. Yttrium Labelled complementary-determining region-grafted monoclonal antibodies for radioimmunotherapy: Radiolabeling and animal biodistribution studies. *Bioconjugate. Chem.* **1998**, *90*, 773-782.
- 65) Kumar Krishan and Tweedle M.F. Ligand and Rigidity Control Formation of Macrocyclic Polyamino Carboxylate Complexes of Gadolinium (III), *Inorg. Chem.* **1993**, *32*, 4193-4199.

- 66) Kasprzyk, S.P.; Wilkins, R.G. Kinetics of interaction of metal ions with two tetraazatetraacetate macrocycles; *Inorg. Chem.* 1982, 21, 3349.
- 67) Kolat, R.S.; Powell, J.E. *Inorg. Chem.* 1962, 1, 485.
- 68) Moller, T.; Moss, F.A.J.; Marshall, R.H. Observations on the Rare Earth. LXVI. Some characteristics of Ethylene- diaminetetraacetic Acid Chelates of certain Rare Earth Metal Ions.; *J. Am. Chem. Soc.* 1955, 77, 3182.
- 69) Nynsen, G.A.; Margerum, D.W. Multidentate ligand kinetics. XVI. Formation and dissociation kinetics of rare earth-cyclohexylenediaminetetraacetate complexes.; *Inorg. Chem.* 1970, 9, 1814.
- 70) Brucher, E.; Sherry A.D. *Inorg. Chem.* 1990, 29, 1555.
- 71) Wang, X.; Tianzhu, J; Comblin, V.; LopezMut, A.; Merciny, E; Desreux, J.F. *Inorg. Chem.* 1992, 31, 1095.
- 72) Brucher, E.; Cortes, S.; Chavez, F.; Sherry, A.D. *Inorg. Chem.* 1991, 30, 2092.
- 73) Sudmier, J.L.; Reilly, C.N. Nuclear Magnetic Resonance Studies of Protonation of some Polyaminocarboxylate compounds containing Asymmetric Carbon Atoms. *Anal. Chem.* 1964, 36, 1707.
- 74) Cossy, C.; Helm, L.; Merbach, A.E. Oxygen-17 nuclear magnetic resonance kinetic study of water exchange on the lanthanide (III) aquaions. *Inorg. Chem.* 1988, 27, 1973.
- 75) Dischino, D.D.; Delaney, E.J.; Eeswiler, J.E.; G.T. Gaughan J.S. Prasad, Srivastava S.K. and Tweedle, M.F. Synthesis of Nonionic Gadolinium Chelates Useful as Contrast Agents for Magnetic Resonance Imaging. 1,4,7-Tris (carboxyl methyl)-10- Substituted-1, 4, 7, 10- tetraazacyclododecanes and Their Corresponding Gadolinium Chelates. *Inorg. Chem.* 1991, 30, 1265-1269.
- 76) Desreux, J.F. *Inorg. Chem.* 1980, 19, 1319
- 77) Kumar Krishan; Tianzhu Jin; Wang Xiangyun; Desreux Jean F.; and Tweedle, M.F. Effect of Ligand Basicity on the Formation and Dissociation Equilibria and Kinetics of  $Gd^{3+}$  Complexes of Macrocylic Polyamino carboxylates; *Inorg. Chem.* 1994, 33, 3823-3829.
- 78) Tse, P.K.; Powell, J.E.; *Inorg. Chem.* 1985, 24, 2727.

- 79) Brucher, Cortes, S; Chavez, F.; Sherry, A.D. Synthesis, equilibrium, and kinetic properties of the gadolinium(III) complexes of three triazacyclodecanetraacetate ligands. *Inorg.Chem.* **1991**, *30*, 2092.
- 80) Lehn, J-M.; Sauvage, J.P.; Cryptates. XVI. [2]-Cryptates. Stability and selectivity of alkaline-earth macrobicyclic complexes. *J. Am.Chem.Soc.* **1975**, *97*, 6700.
- 81) Kang, S.I.; Ranganathan, R.S.; Emawiller, J.E.; Kumar, K.; Gougoutas, J.Z.; Malley, M.; Tweedle, M.F. Synthesis, characterization, and crystal structure of the gadolinium (III) chelate of (1R,4R,7R)- $\alpha$ , $\alpha$ '-trimethyl-1,4,7,10-tetraazacyclododecane-1, 4,7-triacetic acid (DO3MA). *Inorg.Chem.* **1993**, *32*, 2912.
- 82) Kumar Krisshan; Tweedle M.F.; Malley, M.F.; and Gougoutas Z.J. Synthesis Stability, and Crystal Structure Studies of Some  $\text{Ca}^{2+}$ ,  $\text{Cu}^{2+}$ , and  $\text{Zn}^{2+}$  Complexes of Macrocyclic Polyamino Carboxylates. *Inorg. Chem.* **1995**, *34*, 6472-6480.
- 83) Kumar, K.; Chang, C.A., Tweedle, M.F. *Inorg.Chem.* **1993**, *32*, 4193.
- 84) Kumar, K., Jin, T., Wang, X., Desreux, J.F., Tweedle, M.F., *Inorg.Chem.* **1994**, *33*, 33567.
- 85) Brucher, E.; Sherry, A.D.; *Inorg.Chem.* **1990**, *29*, 1555.
- 86) Kodama, M; Koike, T.; Mahatma, A.B.; Kimura, E. *Inorg.Chem.* **1991**, *30*, 1270
- 87) Chandra Sekhar; Chang, C.A. *Inorg.Chem.* **1986**, *26*, 2061.
- 88) Carvalho, J.F.; Kim S-H.; Chang, C.A. *Inorg.Chem.* **1992**, *31*, 4065.
- 89) Delgado, R.; Sun, Y.; Motekaitis, R.J.; Martell, A.E. *Inorg.Chem.* **1993**, *32*, 3320
- 90) Rizkalla, E, N.; Chopping, G.R.; Cacheris, W.P. *Inorg.Chem.* **1993**, *32*, 582.
- 91) Barnett, B.L.; Uctman, V.A. *Inorg.Chem.* **1979**, *18*, 2674.
- 92) Rebizak Richard, Michel Schaefer; Dellacherie E'dith, Polymeric Conjugates of  $\text{Gd}^{3+}$ -Diethylenetriaminepentaacetic Acid and Dextran. 1. Synthesis, Characterization, and Paramagnetic Properties. *Bioconjugate.Chem.* **1997**, *8*, 605-610.

- 93) Armitage, F.E., Richardson, D.E., Li, K.C.P. Polymeric contrast agents for magnetic resonance imaging : synthesis and characterization of gadolinium diethylenetriaminepentaacetic acid conjugated to polysaccharides. *Bioconjugate Chem.* **1990**, *1*, 365-74.
- 94) Rebizak Richard, Michel Schaefer, Dellacherie E'dith. Polymeric Conjugates of  $Gd^{3+}$ -Diethylenetriaminepentaacetic Acid and Dextran. 2. Influence of Spacer Arm Length and Conjugate Molecular Mass on the Paramagnetic Properties and Some Biological Parameters. *Bioconjugate Chem* **1998**, *9*, 94-99.
- 95) Aime, S. Botta, M.; Ermondi, G.; Fidelli, F.; Uggeri, F. Synthesis and NMRD studies of  $Gd^{3+}$  complexes of macrocyclic polyaminopolycarboxylic ligands bearing  $\beta$ -benzyloxy- $\alpha$ -propionic residues. *Inorg. Chem.* **1992**, *31*, 1100.
- 96) Li Min and Meares Claude F. Synthesis, Metal Chelate Stability Studies, and Enzyme Digest of a Peptide-Linked DOTA Derivative and Its Corresponding Radiolabeled Immunoconjugates. *Bioconjugate Chem.* **1993**, *4*, 275-283.
- 97) Hancock Robert D. and Martell Arthur E. Ligand Design for Selective Complexation of Metal Ions in Aqueous Solution. *Chem. Rev.* **1989**, *89*, 1875
- 98) Esinger J.; Shulman R.G.; Blumberg W.E. Relaxational Enhancement by Paramagnetic Ion Binding in Deoxyribonucleic Acid Solutions, *Nature*. *December* **1961**, *9*, 4806, 963-964.
- 99) Silvio Aime; Alessandro Barge; Castelli Daniela Delli; Fedeli Franco, Mortillaro Armando; Nielsen Flemming U; and Terreno Enzo. Paramagnetic Lanthanide (III) Complexes as pH-Sensitive Chemical Exchange Saturation Transfer (CEST) Contrast Agents MRI Applications, *Magnetic Resonance in Medicine*, **2002**, *47*, 639-648.
- 100) Kobayashi Hisataka; Satomi Kawamoto Jo; Sang-Kyung; Bryant Jr. Henry L; Brechbiel Martin W; Star Robert A.; Macromolecular MRI Contrast Agents with Small Dendrimers: Pharmacokinetic Differences between Sizes and Cores. *Bioconjugate Chem.* **2003**, *14*, 388-394.
- 101) Caravan Peter; Cloutier Normal J.; Greenfield Matthew T.; McDermid Sarah A.; Dunham Stephen U.; Bulte Jeff W.M.; Amedio Jr, John C.; Looby Richard J.; Supkowski Ronald M.; DeW. Horrocks Jr, William McMurry Thomas J.; and Lauffer Randall B. The Interactions of MS-325 with Human Serum Albumin and Its Effect on Proton Relaxation Rates, *J. AM. CHEM. SOC.* **2002**, *12*, 3152-3162.

- 102) Dwek, K.; Nuclear Resonance in Biochemistry, Applications to Enzyme Systems: Clarendon: Oxford, 1973; Chapters 9-11.
- 103) Bloch, T.; Hansen, W.W.; Parkard, M.; *Phys. Rev.* **1948**, 70,474.
- 104) Lanterbur, P, C.; Mendoca Dias, M.H.; Rudin, A.M. In Frontier of Biological Energies Dutton, P.L.; Scarpa, A.; Eds.;Academic:New York,1978,p752
- 105) Brady,T.J.;Goldman,M.R.;Pykett,I.L.;et al.*Radiology (Easton,Pa)***1982**,144-343
- 106) Brady, T.J.; Goldman, M.R.; Pykett, I.L.; et al.*Circulation*, **1982**,66,1012.
- 107) Young, I.R., Clark.G.J. Gailes, D.R.; et al.*Comp.Tomogr.***1981**, 5,534.
- 108) Carr,D.H.; Brown,J.;Bydder,G.R.;et al. *Lancet* **1984**,1,484.
- 109) Burton,D.R.;Forsen,S.;Karlstrom,G.;Dwek,R.A.;*Prog.Nucl.Magn.Reson. Spectrosc.***1979**,13,1.
- 110) Luz,Z.; and Meiboom,S. *J.Chem.Phys.***1964**,40,2686.
- 111) Swift, T.J.; Connick, R.E. *J. Chem.Phys.***1962**, 37,307.
- 112) Bloembergen, N.; Purcell, E.M., Pound, R.V. *Phys.Rev.***1948**, 73,678.
- 113) Solomon,I., *Phys.Rev.***1955**,99,559.
- 114) Kowaleski,J.;Nordenskiold,L.;Benetics,N.Westlands,P.O.;*Prog.Nucl.Magn. Reson .Spectrosc.***1985**, 141-185.
- 115) Bertini,L.;Lucichinact.,C. *Cord.Chem.Rev.***1996**,150,1-295.
- 116) Banci,L.;Bertini,I.;Luchinat,C.;Nuclear and Electron Relaxation, *VCH; Weinheim.* **1991** .
- 117) Freed, J.; *J.Chem.Phys.***1978**, 68, 4034.
- 118) Pfeifer, H.*Ann.Phys. (Liezig)* **1961**, 8, 1.
- 119) Bennett, H.F.; Bown, R.D.; Koenig, S.H.; Swartz, H.M. *Magn. Reson.Med.* **1987**,4,93.
- 120) Franano, .N. Edwards,W.B.; Welch,M.J.Brechbiel ,M.W.,Gansow.O.A.; Duncan, J.R. *Magn.Reson. Imaging.***1995**, 15, 13,201-14.
- 121) Wedeking, P., Tweedle, M. *Nucl.Biol.***1988**, 15,395-402.

- 122) Wedeking, P., Kumar, K., Tweedle, M.F. *Nucl.Biol.* **1993**, *20*,679-91.
- 123) Jackson.G.E; Wynchank, S.; and Woundenberg, M. Gadolinium(III) complex equilibria: the implications for Gd(III)MRI contrast agents. *Magn. Reson.Med.* **1990**, *16*, 57-66.
- 124) Sherry,A.D.; Coscharis,W.P.; and Kuank, K,-T. Stability constants for  $Gd^{3+}$  binding to model DTPA- protein:implications for use as magnetic resonance contrast agents. *Magn.Reson.Med.*, **1988**,*8*,180-90.
- 125) Pulukkody, K.P.; Norman,T.J.;Parker,D.,Royle,L.; and Groan,C.J. Synthesis of charged and uncharged complexes of Gadolinium and yttrium with cyclic polyazaphosphinic acid ligands for in vivo applications. *J.Chem. Soc. Perkin. Trans.* 605-620.
- 126) Cox, J.L.; Craig, A.S.; Helps, I.M.; Jankowski, K.J.; Parker.D. Eaton, M.A.W.; Millcan,A T.; Millar,K.; Beeley, B.A. Synthesis of C-and N-functional derivatives of 1,4,7,10-tetraazacyclononane-1,4,7-triacetic acid (NOTA).1,4,7,10- tetraazacyclododecane-1,4,7-tetraacetic acid (DOTA) and diethylenetriaminepentaacetic acid (DTPA):Bifunctional complex agents for the dericvatization of antibodies. *J.Chem.Soc.Perkin Trans.* **1990**, 2567-2576.
- 127) Broan,C.J.; Cox,JP.L.;Craig,A,C.; Katakya,R.; Parker, D.;Harrison,A., Randall,A.M.; and Ferguson,G. Structure and stability of indium and gallium complexes of, 7,10-tetraazacyclononane-1,4,7- triacetic acid (NOTA).and yttrium complexes of 1,4,7,10-tetraazacyclododecane-1,4,7-tetraacetic acid and related ligands kinetically stable complexes for use in imaging and radioimmunotherapy. X-rays molecular structure of the indium and gallium complexes of 1,4,7,10-tetrazacyclononane-1,4,7-triacetic acid. *J.Chem.Soc.Perkin.Trans.* **1991**, 87-99.
- 128) Parker ,D.;Pulukkody,K.P.;Norman,T.J.; Harrison, A., Royle ,L.;and Walker, C. Stable anionic, neutral and cationic complexes of gadolinium with functionalized aminophosphinic and macrocyclic ligands.*J.Chem. Soc.Commun.* **1992**, 1441-1443.
- 129) Goeckerler, W.F.; Edwards,B.;Volkert,W.A.;Holmes,R.A.,Simon,J.,and Wilson, D. Skeletal localization of samarium-153 chelates: potential therapeutic bone agents. *J.Nucl.Med.* **1987**, *28*,495-504.
- 130) Goecker,W.F.;Troutner,D.E.,Volker,W.A.;Edwards,B.,Simon,J.and Wilson, D.153Sm radiotherapeutic bone agents. *J. Nucl.Med.Biol.* **1986**, *13*,479-482.

- 131) Atkins, H.L.; Mausner, L.F.; Srivassta, S.C.; Meinken, G.E.; Straub, R.F.; Cabahug, C.J.; Weber, D.A.; Wong, C.T.; Sacker, D.F.; Madajewicz, S.; Parker, T.L.; and Meek, A. G. Biodistribution of Sn117m (4+) DTPA for palliative therapy of painful osseous metastasis. *Radiology*. 186,279-283.
- 132) Kumar, K.; Tweedle, M.F. *Inorg. Chem.* 1993, 32, 4193-4199.
- 133) Bruchner, E.; Sherry, A.D. *Inorg. Chem.* 1990, 29,1555-1559.
- 134) Lewis, M.R.; Raubitschek, A.; and Shively, J.E. A facile, water soluble method for modification of proteins with DOTA. Use of elevated temperature and optimized pH to achieve high stability in radiolabeled immunoconjugates. *Bioconjugates. Chem.* 1994, 5,565-576.
- 135) Lewis, M.R.; and Shively, J.E. Maleimidocytteimino-DOTA derivatives: New reagents for radiometal chelates conjugates to antibody sulfhydryl groups undergo pH dependent cleavage reactions. *Bioconjugate.Chem.* 1998,9, 72-86.
- 136) Delgado, R.; and Frausto daSilva, J.J.R. Metal complexes of cyclic tetra-azatetraacetic acids. *Talanta.*, 29,815-822.
- 137) Clark, E.T.; and Martel, A.E. Stabilities of the alkaline earth and divalent transition metal complexes of the tetraazamacrocyclic tetraacetic acid ligands. *Inorg. Chim. Acta.* 190.19,324.
- 138) Wolf, G.L.; Forben, E.S. *Invest. Radiol.* 1984, 19,324.
- 139) Lauffer, R.B.; Vincent, A.C.; Padmanabhan, S.; Villringer, A.; Saini, S., Elmalch, D.R.; Brady, T.J. *Magn. Reson. Med.* 1987, 4,582.
- 140) Dellacherie, E.; In Polysaccharides in Medicinal Applications. Dumitriu.S. Ed.; Marcel Derkker; *New York*, 1996.
- 141) Casali, C.; Janier, M.; Canet, E.; Obadia, J.F.; Benderbous, S.; Carot, C.; Revel, D. *Acad. Radiol.* 1998, 5, S214- S218.
- 142) Tomalia, D.; Naylor, A.; Goddard, W.; III. *Angew. Chem. Int. Ed. Engl.* 1990, 29,138-175.
- 143) Tomalia, D.A.; Durst, H.D. *Top. Curr. Chem.* 1993, 165,193-313.
- 144) Atkins Peter. The Elements of Physical Chemistry With Applications in Biology .W.H.Freeman and Company, New York, 3<sup>rd</sup> Ed, 2001, pp. 459-473.

I, Samuel Robert Smith Sarsah, submit this thesis to Emporia State University as partial fulfillment of the requirements for the Master of Science degree in chemistry. I agree that this thesis will be made available for use by the University library according to the standards and regulations governing the usage of such documents. I also agree that any act regarding quoting, photocopying, or reproduction of this document is permitted for private study, scholarship (including teaching) or research for non-profit purposes. Copying or reproduction of any part of this document for financial gain will not be allowed without written permission of the author.



---

Signature of Author

06/01/2005

---

Date

DESIGN AND SYNTHESIS OF AN  
OLIGONUCLEOTIDE-DOTA CONJUGATE

---

Title of Thesis



---

Signature of Graduate Office Staff

6-2-05

---

Date Received